Gravitational wave evolution from acoustic and vortical sources

- Pencil Code
- Correspondence between kinetic or magnetic spectra with GW spectra
- Inertial and subinertial range spectra
- Scalar and vector modes in vertical and acoustic (irrotational) turbulence
- Onset of GW energy and vorticity

Axel Brandenburg, Tina Kahniashvili, Arthur Kosowsky,
Sayan Mandal, & Alberto Roper Pol

History of gravitational waves

- Heaviside (1893): analogy with electromagnetism
- Poincare (1905): emanating from body at speed of light
- Einstein (1916, 1918), three types of waves
- Eddington (1922): two of three are artifacts
- Einstein & Rosen (1936) unphysical altogether
- referee Robertson: harmless coordinate singularities
- Pirani (1956): manifestly gauge-invariant observables
- Hulse & Taylor (1975): → indirect GW detection
- GW150914. 2017 Nobel prize to Weiss, Thorne, Barish

Confused situation by 1936

July 27, 1936

Dear Sir.

"We (Mr. Rosen and I) had sent you our manuscript for publication and had not authorized you to show it to specialists before it is printed. I see no reason to address the—in any case erroneous—comments of your anonymous expert. On the basis of this incident I prefer to publish the paper elsewhere."

Respectfully

Einstein

An anecdote illustrating the confused situation prevailing at that time is given in Infeld's autobiography. Infeld refers to the day before a scheduled talk that Einstein was to give at Princeton on the "Nonexistence of gravitational waves." Einstein was already aware of the error in his manuscript, which was previously pointed out by Infeld. There was no time to cancel the talk. The next day Einstein gave his talk and concluded, *"If you ask me whether there are gravitational waves or not, I must answer that I don't know. But it is a highly interesting problem"* [10].

"Note—The second part of this article was considerably altered by me after the departure to Russia of Mr. Rosen as we had misinterpreted the results of our formula. I want to thank my colleague Professor Robertson for their friendly help in clarifying the original error. I also thank Mr. Hoffmann your kind assistance in translation."

In the end, Einstein became convinced of the existence of gravitational waves, whereas Nathan Rosen always thought that they were just a formal mathematical construct with no real physical meaning.

EVIDENCE FOR DISCOVERY OF GRAVITATIONAL RADIATION*

J. Weber
Department of Physics and Astronomy, University of Maryland, College Park, Maryland 20742
(Received 29 April 1969)

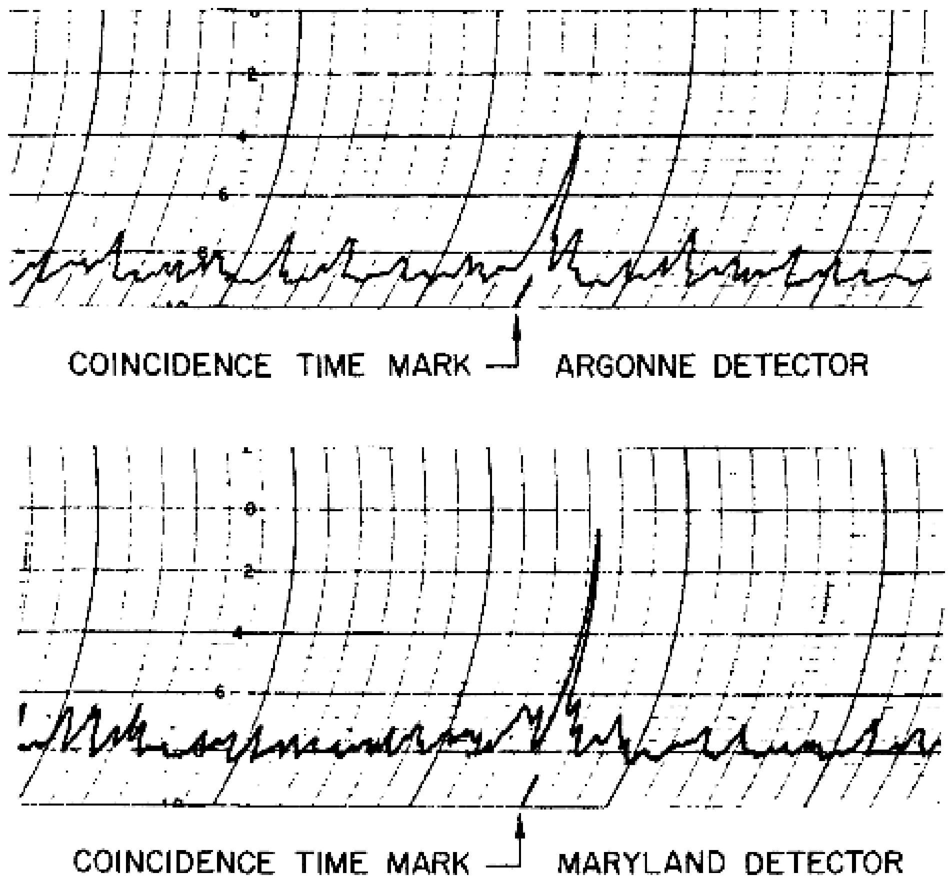

FIG. 2. Argonne National Laboratory and University of Maryland detector coincidence.

Stretching of space-time

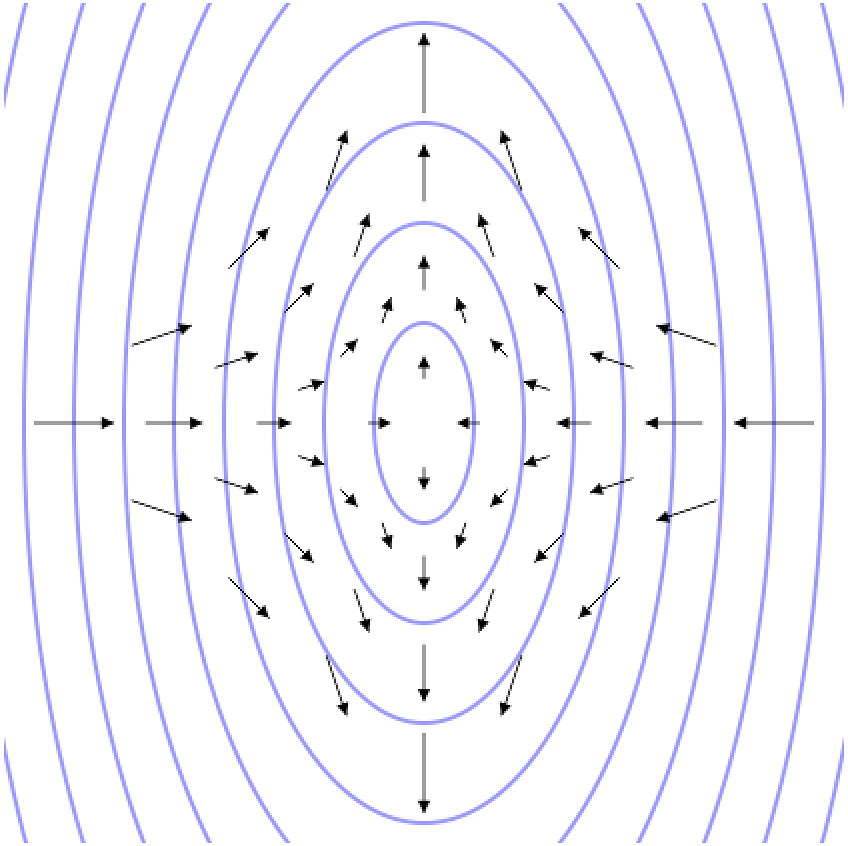

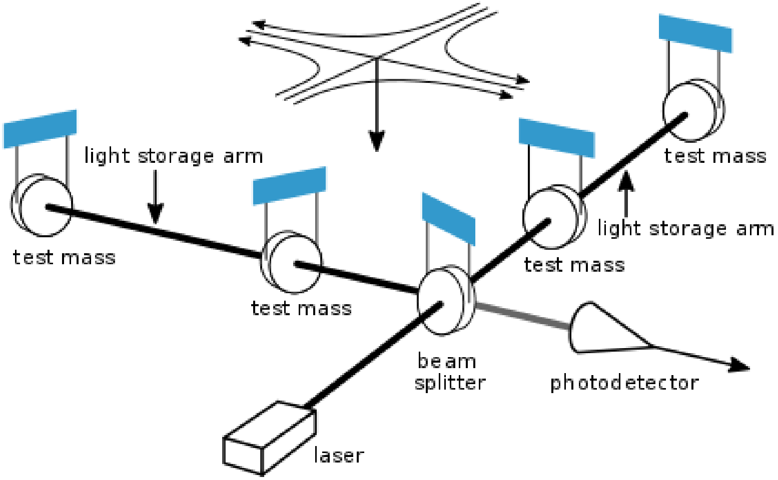

Cosmological GWs

Amplification of gravitational waves in an isotropic universe

L. P. Grishchuk

State Astronomical Institute
(Submitted April 1, 1974)
Zh. Eksp. Teor. Fiz. **67**, 825–838 (September 1974)

It is shown that weak gravitational waves in a nonstationary isotropic universe can be amplified to a greater degree than indicated by the adiabatic law. It is a necessary (but not a sufficient) condition for the amplification that there should exist such a stage in the evolution of the universe when the characteristic time for change in the background metric is less than the period of the wave. In an expanding universe the wave is the more amplified the more strongly does the rate of evolution of the universe differ from the one which is dictated by matter with the equation of state $p=\epsilon/3$, and the earlier the wave had been "started." The superadiabatic amplification of gravitational waves denotes the possibility of creation of gravitons. An exceptional position is occupied by the "hot" isotropic universe with $p=\epsilon/3$, in which the superadiabatic amplification of gravitational waves and the production of gravitons is impossible. An estimate is made of the converse reaction of the gravitons on the background metric. Apparently, the production of gravitons forbids at least those of the iostropic singularities near which $p>\epsilon/3$.

VOLUME 69, NUMBER 14 PHYSICAL REVIEW LETTERS 5 OCTOBER

Gravitational Waves from First-Order Cosmological Phase Transitions

Arthur Kosowsky,[1],[2] Michael S. Turner,[1],[2],[3] and Richard Watkins[1],[3]

[1]*NASA/Fermilab Astrophysics Center, Fermi National Accelerator Laboratory, Batavia, Illinois 60510-0500*

[2]*Department of Physics, Enrico Fermi Institute, The University of Chicago, Chicago, Illinois 60637-1433*

[3]*Department of Astronomy & Astrophysics, Enrico Fermi Institute, The University of Chicago, Chicago, Illinois 60637-I*

(Received 6 December 1991; revised manuscript received 26 May 1992)

A first-order cosmological phase transition that proceeds through the nucleation and collision of true-vacuum bubbles is a potent source of gravitational radiation. Possibilities for such include first-order inflation, grand-unified-theory-symmetry breaking, and electroweak-symmetry breaking. We have calculated gravity-wave production from the collision of two scalar-field vacuum bubbles, and, using an approximation based upon these results, from the collision of 20 to 30 vacuum bubbles. We present estimates of the relic background of gravitational waves produced by a first-order phase transition; in general, $\Omega_{GW} \sim 10^{-9}$ and $f \sim (10^{-6}\ \text{Hz})(T/1\ \text{GeV})$.

EW D VOLUME 45, NUMBER 12

Gravitational radiation from colliding vacuum bubbles

Arthur Kosowsky, Michael S. Turner, and Richard Watkins

/Fermilab Astrophysics Center, Fermi National Accelerator Laboratory, Batavia, Illin
and Departments of Physics and Astronomy & Astrophysics, Enrico Fermi Institu
The University of Chicago, Chicago, Illinois 60637-1433

(Received 20 December 1991)

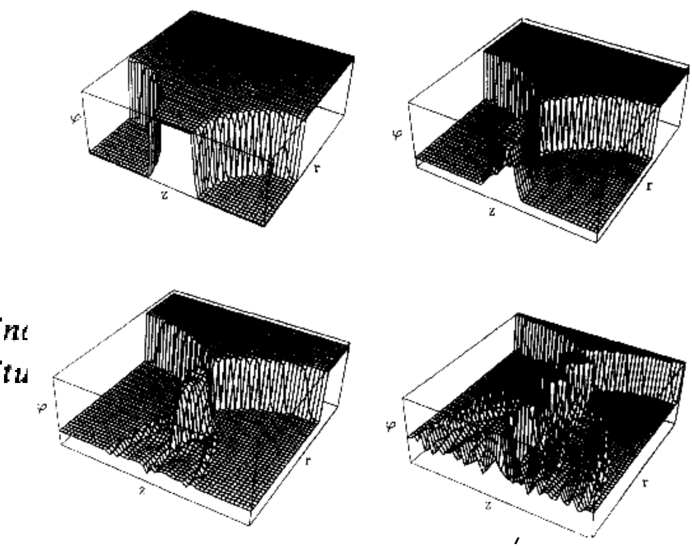

Why interesting if random?

- Energy spectrum
  - Peak(s)
  - Slopes
  - Relation to turbulence
- Polarization
  - Sign?
  - Relation magnetic helicity (=swirl of B field)

Solve for spatial part of h_{ij}

- Sourced by the stress tensor (Reynolds, Maxwell)
  - T_{ij} is symmetric tensor
  - 6 components
- Assume transverse $dT_{ij}/dx_j = 0$
  - 3 constraints
  - 3 components left
- Traceless
  - 1 more constraint
  - 2 components left

Correspond to + and x modes

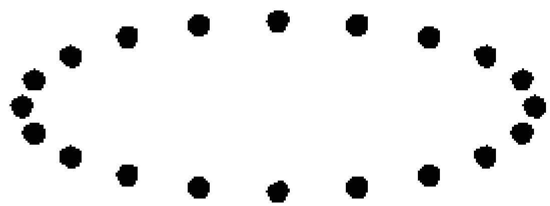

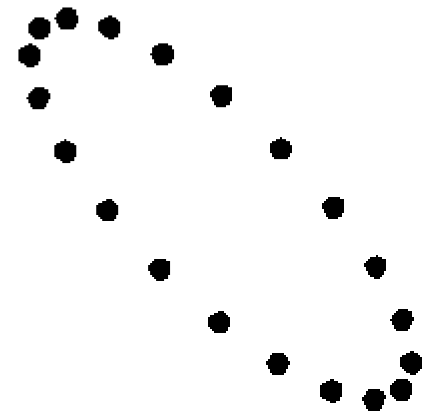

$$\begin{pmatrix} \langle h_+(\boldsymbol{n})h_+^*(\boldsymbol{n}')\rangle & \langle h_+(\boldsymbol{n})h_\times^*(\boldsymbol{n}')\rangle \\ \langle h_+^*(\boldsymbol{n})h_\times(\boldsymbol{n}')\rangle & \langle h_\times(\boldsymbol{n})h_\times^*(\boldsymbol{n}')\rangle \end{pmatrix}$$

$$\frac{\delta_{drc}(\boldsymbol{n}-\boldsymbol{n}')}{4\pi}\begin{pmatrix} I+Q & U-iV \\ U+iV & I-Q \end{pmatrix}$$

Seto (2006)

Circular polarization in space & time

- Both plus and cross polarization together
- Combine the two as a function of space & time
- Get circular polarization

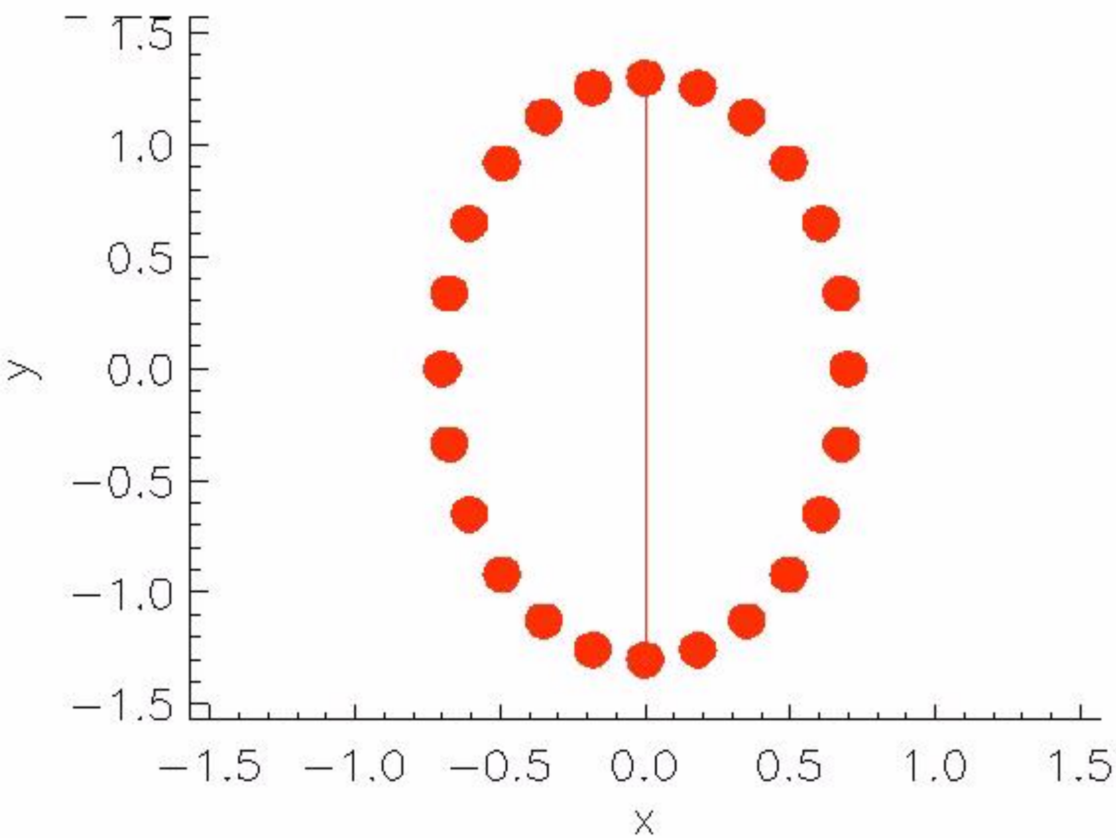

Alfvén wave

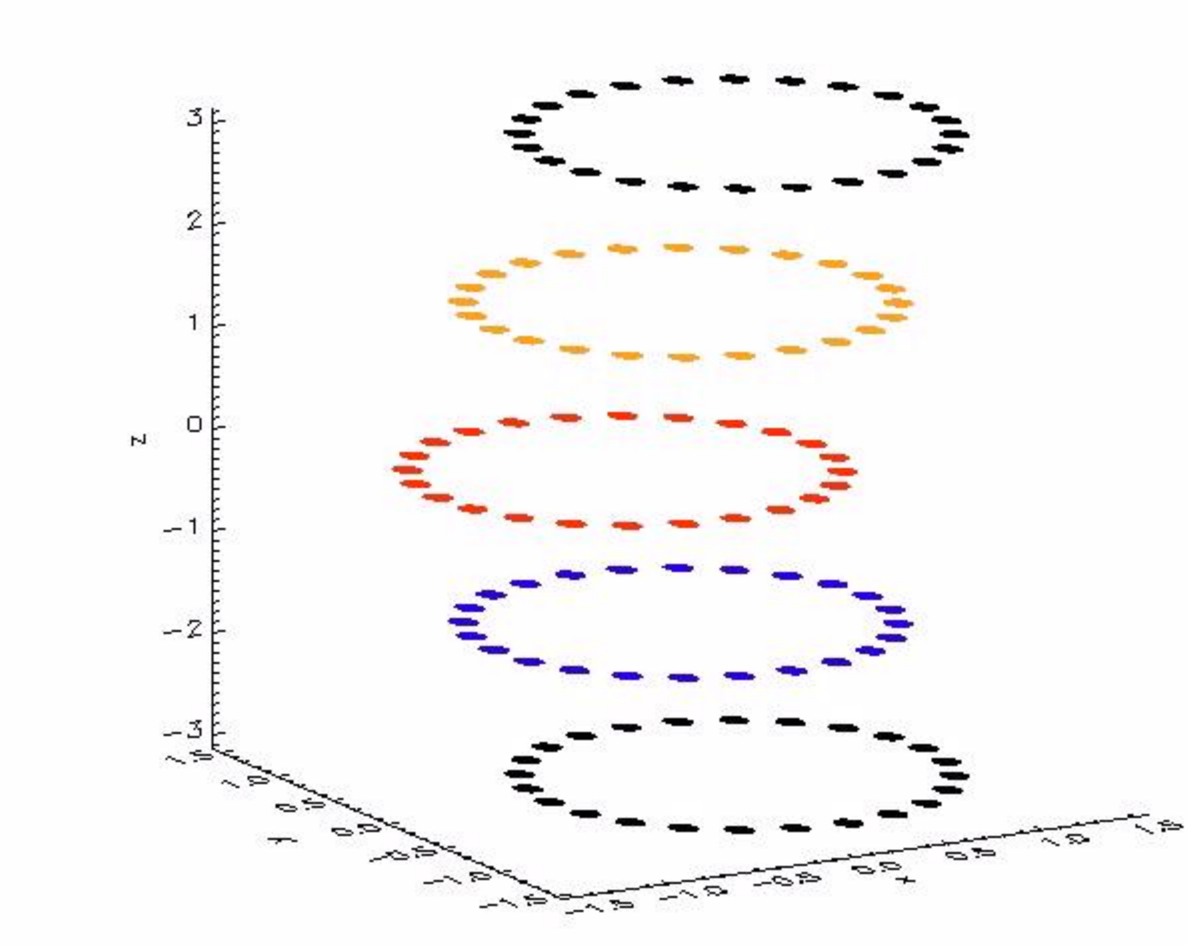

1. travel up
2. travel down
3. standing wave

magnetic fluctuations

Alfvén wave

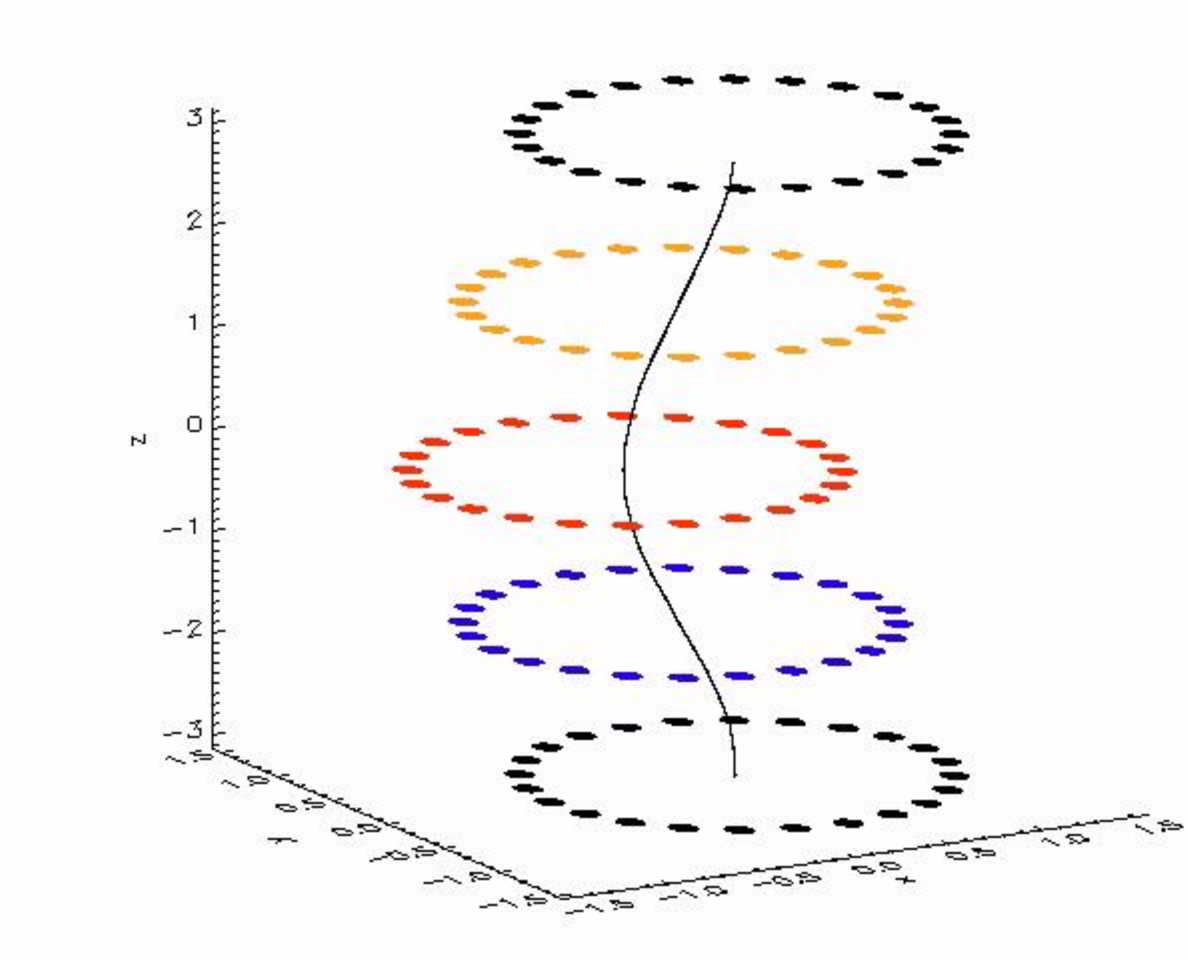

Alfvén wave

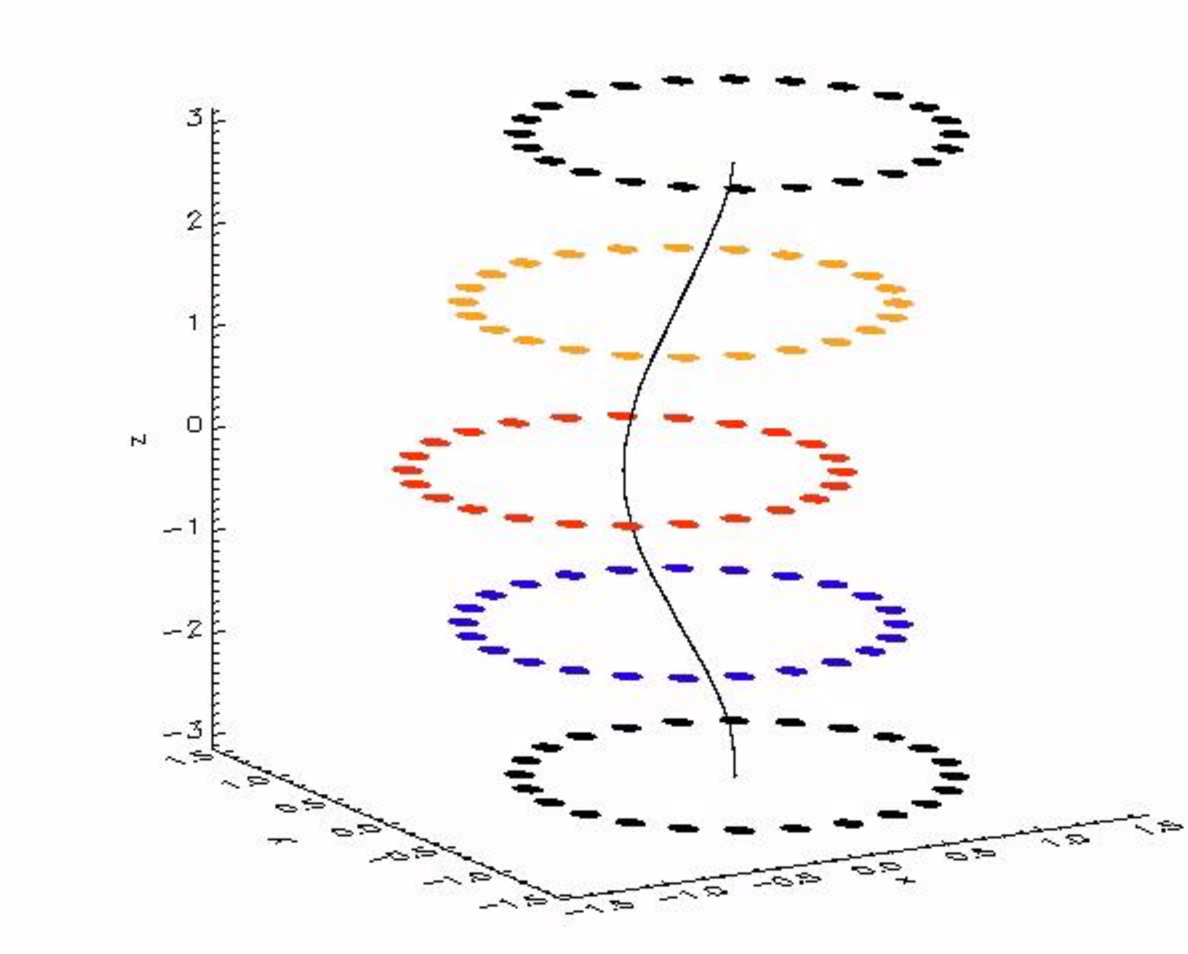

Alfvén wave

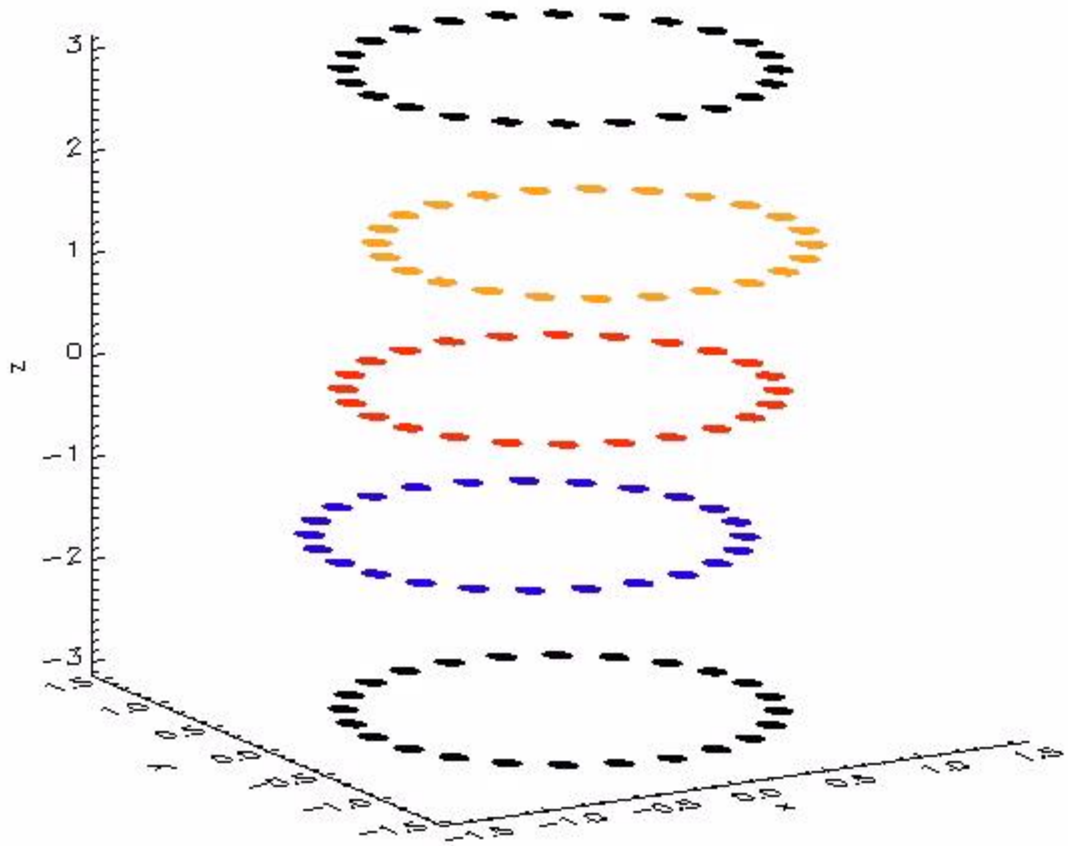

Alfvén wave

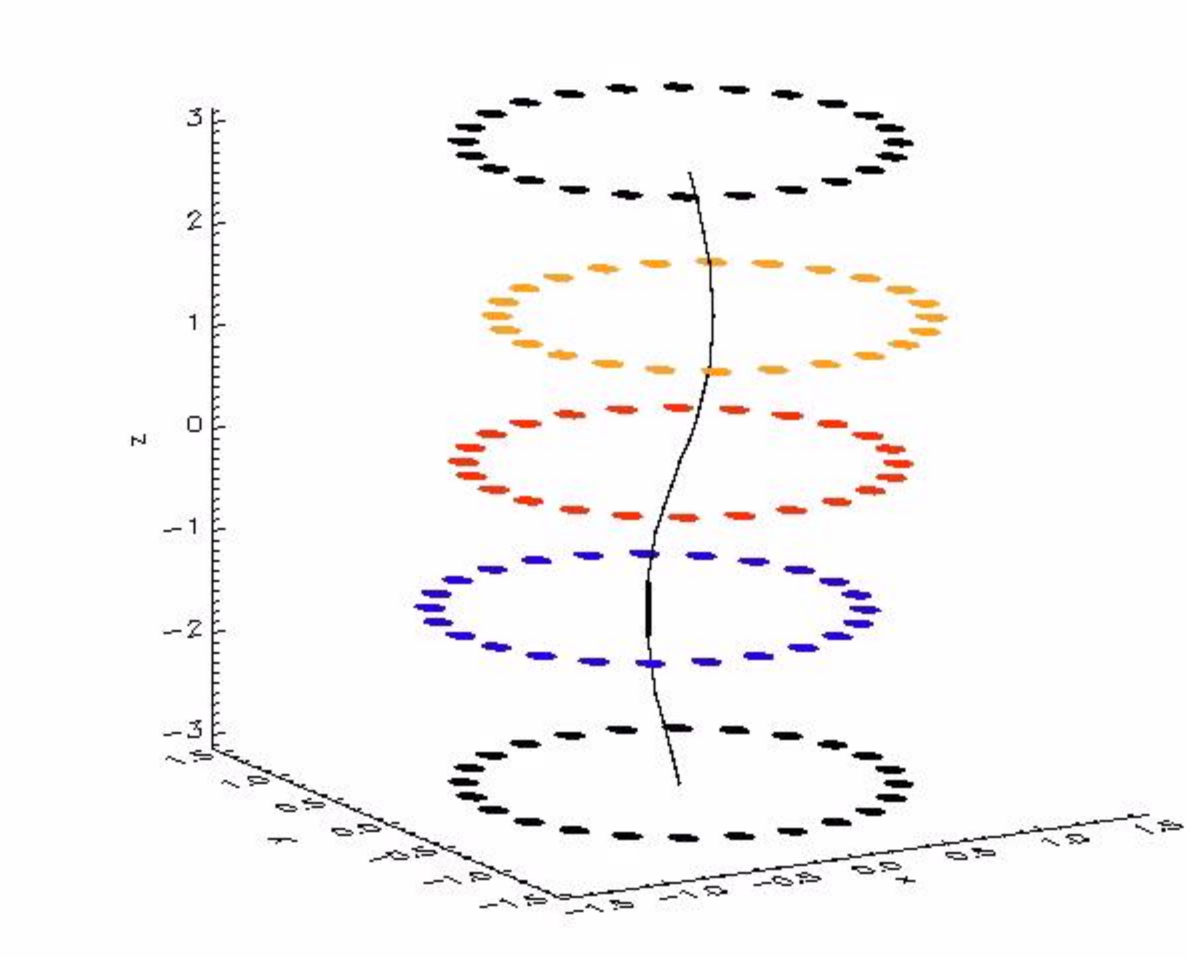

Polariserad Alfvén wave

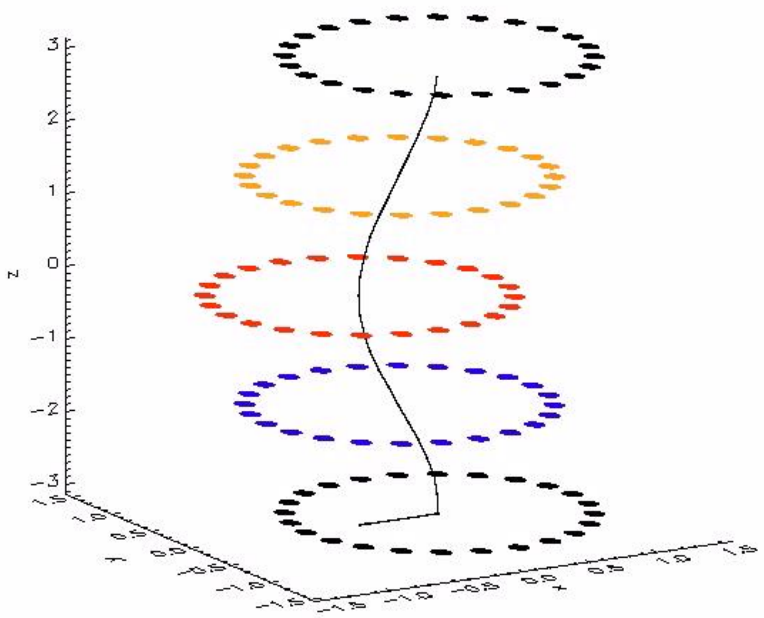

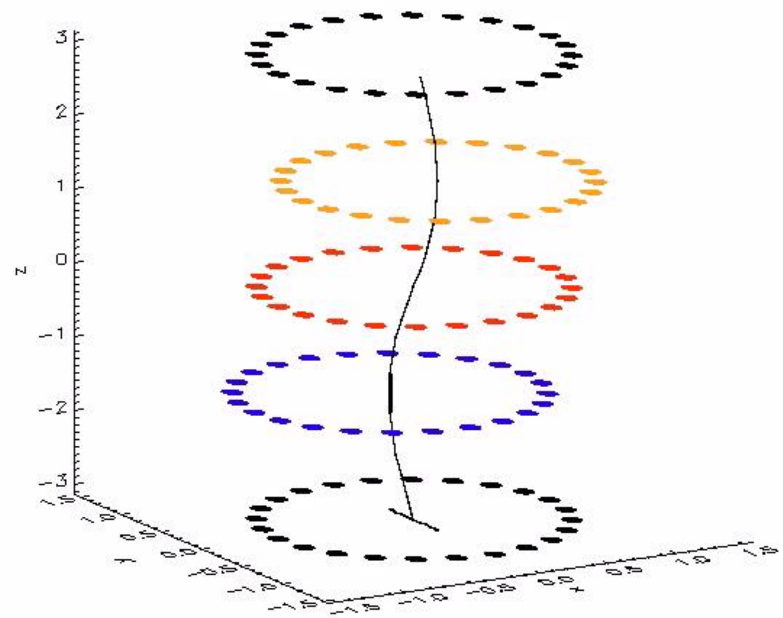

x-polarized

y-polarized

Either x or y

Circularly polarized Alfvén wave

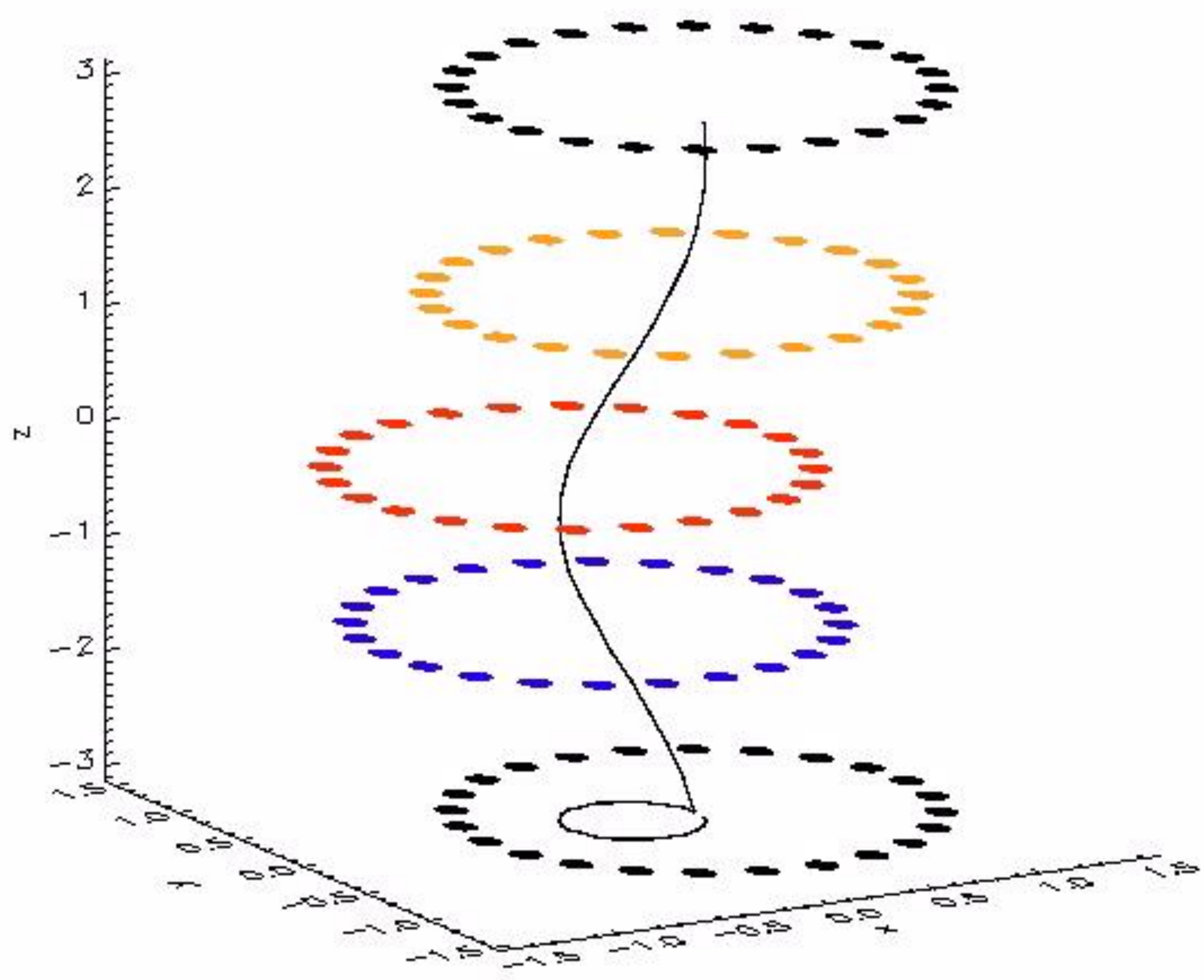

circle

How does it travel?

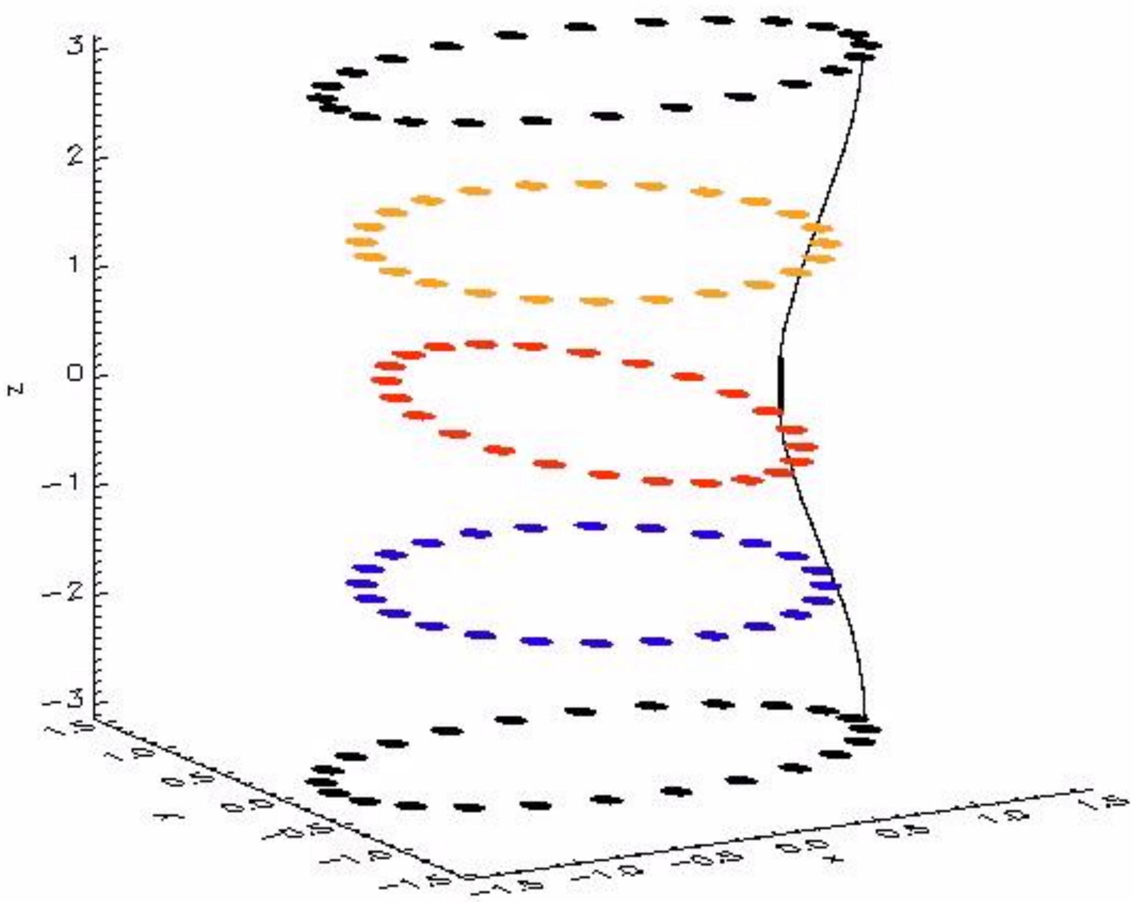

State of the art: stochastic GW from

- MHD turbulence
  - Only analytic models
  - Using Lighthill approximation
- Expanding & colliding bubbles
  - Simulations by Hindmarsh et al. (2015)
  - Solve scalar field dynamics

PHYSICAL REVIEW D **76,** 083002 (2007)

Spectrum of gravitational radiation from primordial turbulence

Grigol Gogoberidze,[1,2,*] Tina Kahniashvili,[3,2,†] and Arthur Kosowsky[4,‡]
[1]*Centre for Plasma Astrophysics, K.U. Leuven, Celestijnenlaan 200B, 3001 Leuven, Belgium*
[2]*National Abastumani Astrophysical Observatory, 2A Kazbegi Ave, GE-0160 Tbilisi, Georgia*
[3]*Center for Cosmology and Particle Physics, New York University, 4 Washington Plaza, New York, New York 10003, USA*
[4]*Department of Physics and Astronomy, University of Pittsburgh, 3941 O'Hara Street, Pittsburgh, Pennsylvania 15260, USA*
(Received 4 May 2007; published 5 October 2007)

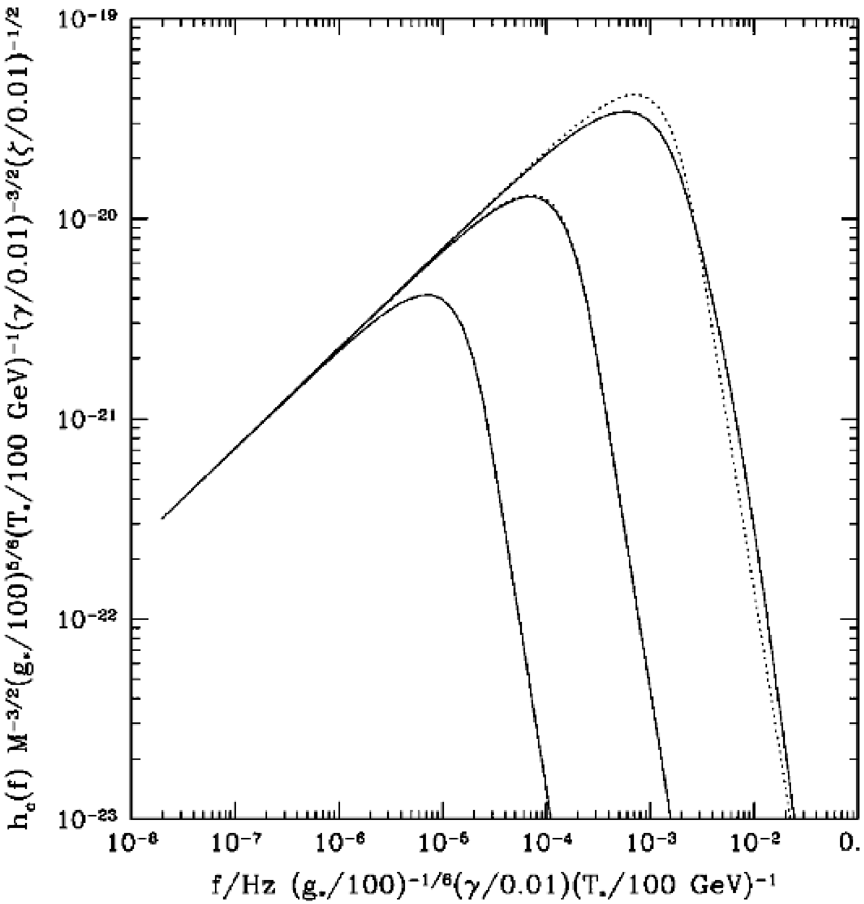

- Kolmogorov turbulence
- Peak at f = 1 mHz
- Lighthill approx.
- $h(f) \sim 3\mathrm{x}10^{-20}$
  - dimensionless

B-field from electroweak PT

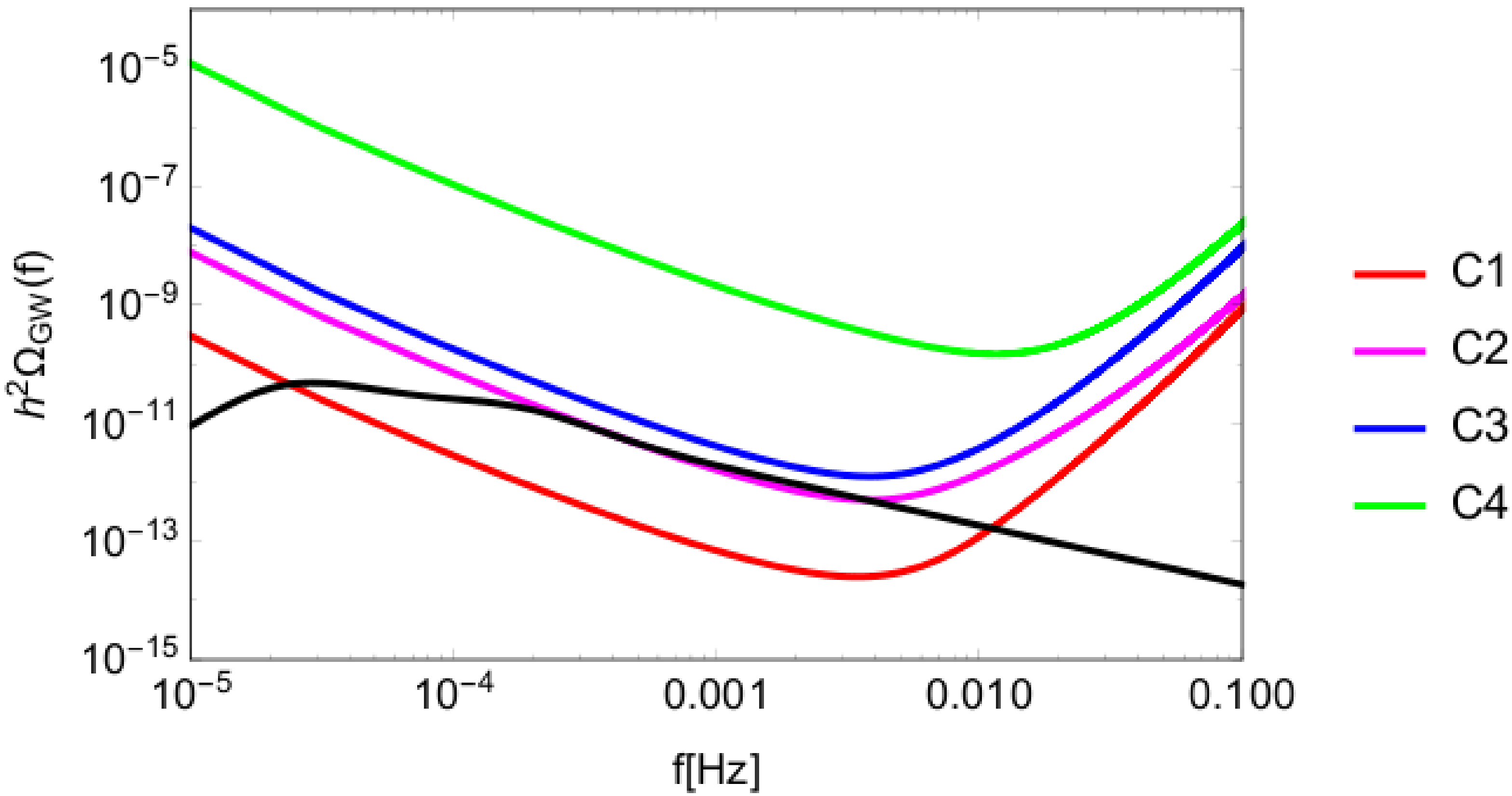

- GW energy normalized by critical energy density
- Around 10^{-10} (nondimensional), at 0.03 mHz

Goal: compute GWs from real MHD turbulence

- Most popular scenario: electroweak phase transition
  - Weak and electromagnetic force decouple
- B-field from electroweak phase transition
  - Vachaspati (1991)
  - Cheng & Olinto (1994)
  - Baym, Bodeker, McLarran (1996)
- Time 10^{-11} sec
  - Horizon scale 0.3 cm
  - Now ~ 10AU → small
  - But turbulence → larger length scale (inverse cascade!)

Relativistic equations in expanding Universe

Energy momentum tensor

Brandenburg, Enqvist, Olesen
Phys Rev D 54, 1291 (1996)

$$T^{\mu\nu}=(p+\rho)U^{\mu}U^{\nu}+pg^{\mu\nu}$$

$$+\frac{1}{4\pi}\left(F^{\mu\sigma}F^{\nu}{}_{\sigma}-\frac{1}{4}g^{\mu\nu}F_{\lambda\sigma}F^{\lambda\sigma}\right),$$

Conformal time, rescaled equations $\mathbf{S}=(p+\rho)\gamma^2\mathbf{v}$

$$\tilde{t}=\int dt/R. \qquad \tilde{\mathbf{S}}=R^4\mathbf{S}, \quad \tilde{p}=R^4p, \quad \tilde{\rho}=R^4\rho, \quad \tilde{\mathbf{B}}=R^2\mathbf{B},$$

$$\tilde{\mathbf{J}}=R^3\mathbf{J}, \quad \text{and} \quad \tilde{\mathbf{E}}=R^2\mathbf{E}.$$

Equivalent to usual magneto-hydrodynamics

$$\frac{\partial\tilde{\mathbf{S}}}{\partial\tilde{t}}=-(\boldsymbol{\nabla}\cdot\mathbf{v})\tilde{\mathbf{S}}-(\mathbf{v}\cdot\boldsymbol{\nabla})\tilde{\mathbf{S}}-\boldsymbol{\nabla}\tilde{p}+\tilde{\mathbf{J}}\times\tilde{\mathbf{B}}.$$

$$\frac{\partial\tilde{\mathbf{B}}}{\partial\tilde{t}}=-\nabla\times\tilde{\mathbf{E}}, \qquad \boldsymbol{\nabla}\cdot\tilde{\mathbf{B}}=0,$$

Small Lorentz factors, γ~1

$$\frac{\partial \ln \tilde{\rho}}{\partial \tilde{t}} = -\frac{4}{3}(\mathbf{v}\cdot\boldsymbol{\nabla}\ln\tilde{\rho} + \boldsymbol{\nabla}\cdot\mathbf{v}) - \frac{\tilde{\mathbf{J}}\cdot\tilde{\mathbf{E}}}{\tilde{\rho}},$$

$$\frac{D\mathbf{v}}{D\tilde{t}} = -\mathbf{v}\left(\frac{D\ln\tilde{\rho}}{D\tilde{t}} + \boldsymbol{\nabla}\cdot\mathbf{v}\right) - \frac{1}{4}\boldsymbol{\nabla}\ln\tilde{\rho} + \frac{\tilde{\mathbf{J}}\times\tilde{\mathbf{B}}}{\frac{4}{3}\tilde{\rho}},$$

where $D/D\tilde{t} = \partial/\partial\tilde{t} + \mathbf{v}\cdot\boldsymbol{\nabla}$ is the total derivative, and

$$\frac{\partial\tilde{\mathbf{B}}}{\partial\tilde{t}} = \nabla\times(\mathbf{v}\times\tilde{\mathbf{B}}), \qquad \tilde{\mathbf{J}} = \boldsymbol{\nabla}\times\tilde{\mathbf{B}}.$$

Magnetohydrodynamic turbulence

The conclusion from the above expressions is thus that *the MHD equations in an expanding universe with zero curvature are the same as the relativistic MHD equations in a nonexpanding universe, provided the dynamical quantities are replaced by the scaled "tilde" variables, and provided conformal time $\tilde{t}$ is used.* The effect of this is, as usual, that

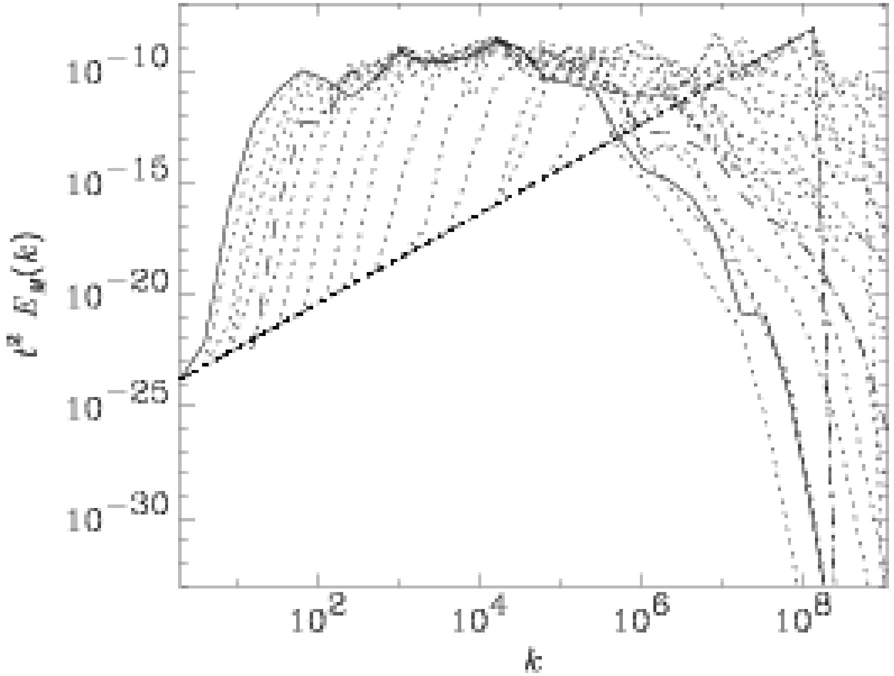

shell models

$$\frac{db_n}{d\tilde{t}} = M_n(v,b)$$

$$\begin{aligned} M_n(v,b) = {} & ik_n(A-C)(v^*_{n+1}b^*_{n+2} - b^*_{n+1}v^*_{n+2}) \\ & + ik_n(B+\tfrac{1}{2}C)(v^*_{n-1}b^*_{n+1} - b^*_{n-1}v^*_{n+1}) \\ & - ik_n(\tfrac{1}{2}B - \tfrac{1}{4}A)(v^*_{n-2}b^*_{n-1} - b^*_{n-2}v^*_{n-1}), \end{aligned}$$

$$\frac{4}{3}\rho_0 \frac{dv_n}{d\tilde{t}} = N_n(v,b)$$

3-D decay simulations

Initial slope
***E~k*⁴**

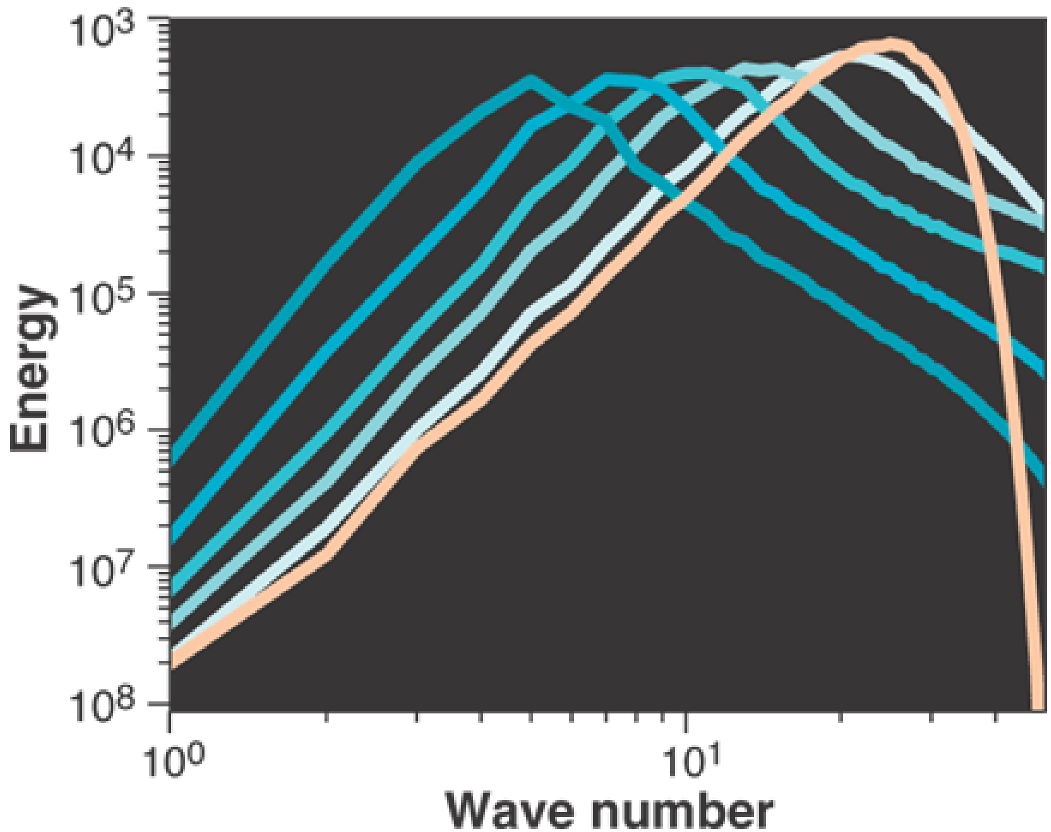

helical vs
nonhelical

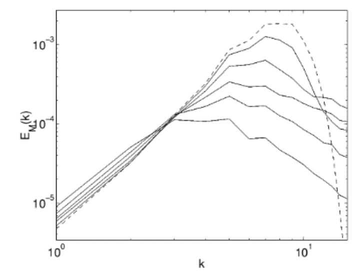

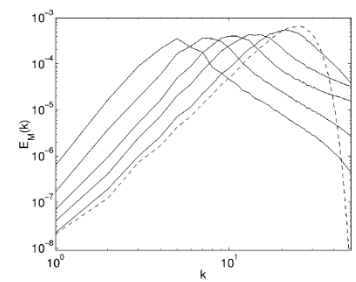

Christensson et al.
(2001, PRE 64, 056405)

Horizon scales for k^4 spectrum

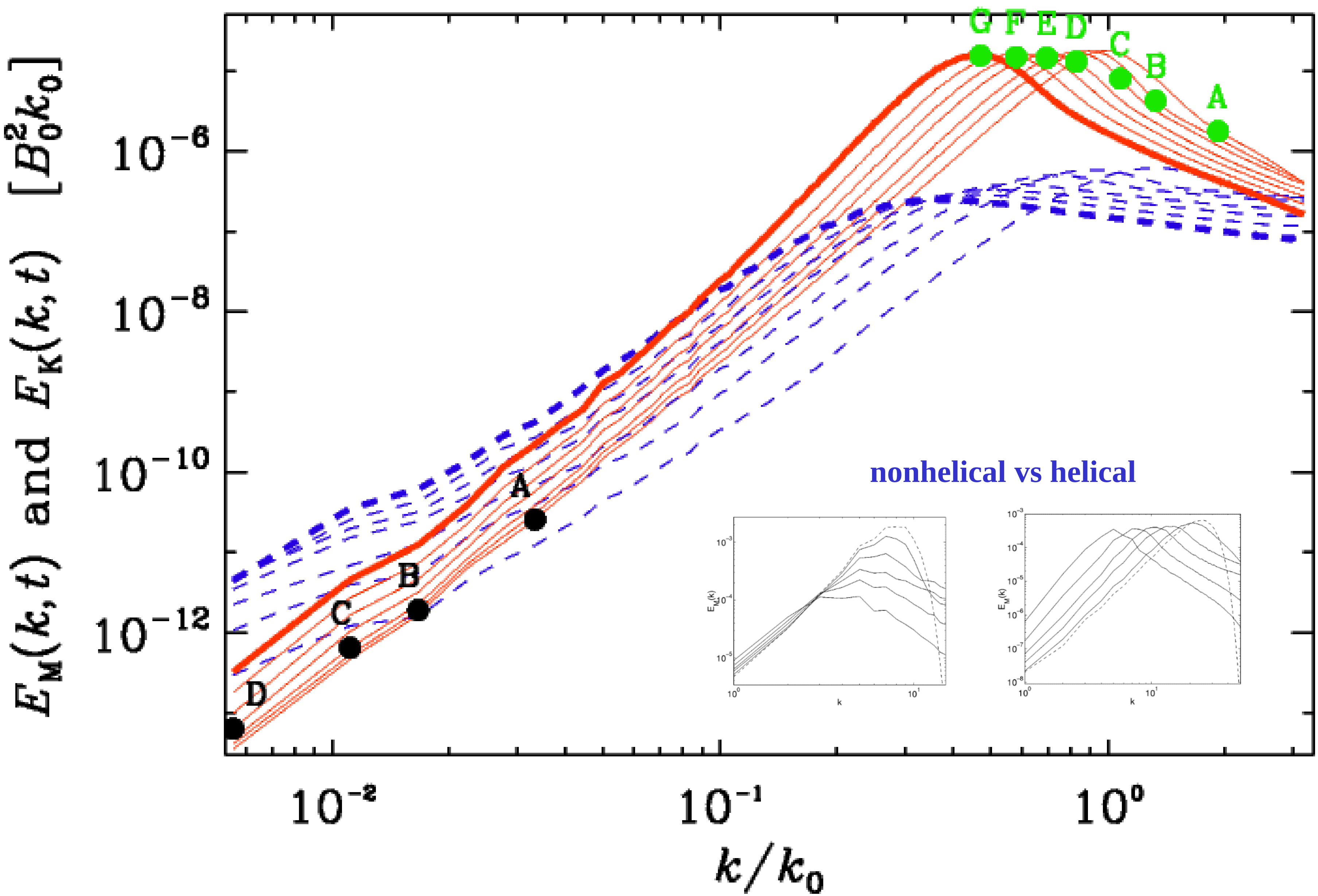

PHYSICAL REVIEW D **70**, 123003 (2004)

Evolution of cosmic magnetic fields: From the very early Universe, to recombination, to the present

Robi Banerjee[1] and Karsten Jedamzik[2]
[1]*Department of Physics and Astronomy, McMaster University, Hamilton, Ontario, Canada L8S 4M1*
[2]*Laboratoire de Physique Mathémathique et Théorique, Université de Montpellier II, 34095 Montpellier Cedex 5, France*
(Received 24 August 2004; published 6 December 2004)

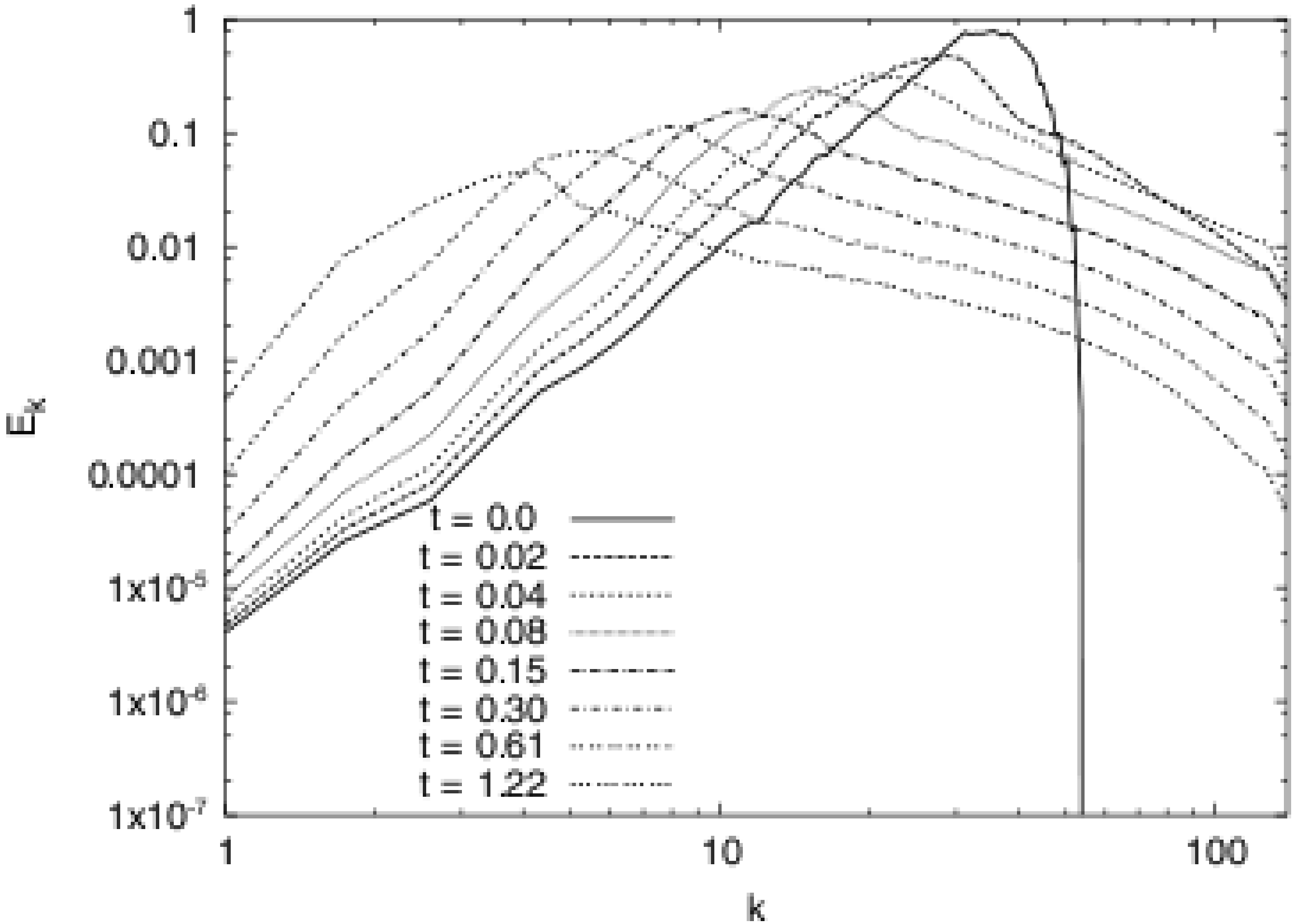

Collapsed spectra and *pq* diagrams

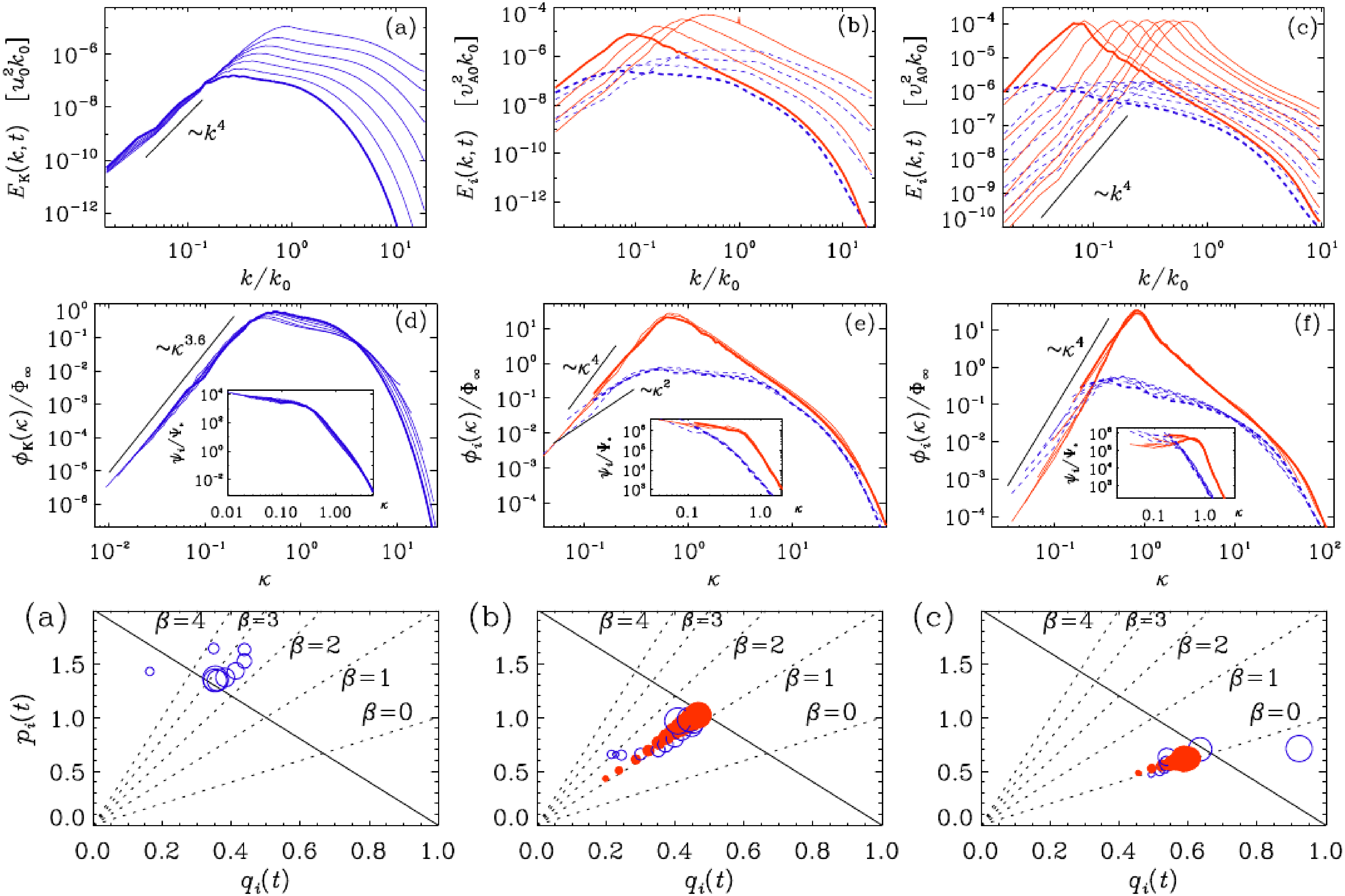

Draft version October 15, 2019
Preprint typeset using LaTeX style emulateapj v. 08/22/09

MAGNETIC HELICITY DISSIPATION IN AN IDEAL MHD CODE

Axel Brandenburg[1,2,3,4] & Evan Scannapieco[5]
[1]Nordita, KTH Royal Institute of Technology and Stockholm University, Roslagstullsbacken 23, SE-10691 Stockholm, Sweden
[2]Department of Astronomy, AlbaNova University Center, Stockholm University, SE-10691 Stockholm, Sweden
[3]JILA and Laboratory for Atmospheric and Space Physics, University of Colorado, Boulder, CO 80303, USA
[4]McWilliams Center for Cosmology & Department of Physics, Carnegie Mellon University, Pittsburgh, PA 15213, USA
[5]Arizona State University, School of Earth and Space Exploration, P.O. Box 871404, Tempe, AZ 85287, USA

(Dated: Revision: 1.66)
Draft version October 15, 2019

ABSTRACT

We study a turbulent helical dynamo in a periodic domain by solving the ideal magnetohydrodynamic (MHD) equations with the `FLASH` code using the divergence-cleaning eight-wave method and compare our results with with direct numerical simulations (DNS) using the Pencil Code. At low resolution, `FLASH` reproduces the DNS results qualitatively by developing the large-scale magnetic field expected from DNS, but at higher resolution, no large-scale magnetic field is obtained. In all those cases in which a large-scale magnetic field is generated, the ideal MHD equations yield too little power at small scales. As a consequence, the small-scale current helicity is too small compared with the DNS. The resulting net current helicity has then always the wrong sign, and it also does not approach zero at late times, as expected from the DNS. Our results have implications for astrophysical dynamo simulations of stellar and galactic magnetism using ideal MHD codes.

This work was performed at the Aspen Center for Physics, which is supported by National Science Foundation grant PHY-1607611. We enjoyed the stimulating atmosphere during the Aspen program on the Turbulent Life of Cosmic Baryons. This research was supported in part by the Astronomy and Astrophysics Grants Program of the National Science Foundation (grants 1615100 and 1715876).

MHD module & forcing

We use the MHD eight-wave module of FLASH (Derigs et al. 2016), which is based on a divergence-cleaning algorithm. The forcing function is analogous to that used by Sur et al. (2014), except that here only one sign of helicity is used. In particular, we used an artificial forcing term F which is modeled as a stochastic Ornstein-Uhlenbeck process (Eswaran & Pope 1988; Benzi et al. 2008) with a user-specified forcing correlation time, which was taken to be one half. In the following, we consider two values for the scale separation ratio k_f/k_1: a smaller one with a combination of 76 wavevectors with wavenumbers between 2 and 3, and a larger one with 156 wavevectors with wavenumbers between 4 and 5. These cases are distinguished by their average nominal forcing wavenumbers of 2.5 and 4.5, respectively.

Contents lists available at ScienceDirect

Journal of Computational Physics

www.elsevier.com/locate/jcp

A novel high-order, entropy stable, 3D AMR MHD solver with guaranteed positive pressure

Dominik Derigs[a,*], Andrew R. Winters[b], Gregor J. Gassner[b], Stefanie Walch[a]

[a] I. Physikalisches Institut, Universität zu Köln, Zülpicher Straße 77, 50937 Köln, Germany
[b] Mathematisches Institut, Universität zu Köln, Weyertal 86-90, 50931 Köln, Germany

A R T I C L E   I N F O

Article history:
Received 21 January 2016
Received in revised form 11 April 2016
Accepted 24 April 2016
Available online 28 April 2016

Keywords:
Magnetohydrodynamics
FLASH
Entropy stable
Finite volume schemes
Pressure positivity

A B S T R A C T

We describe a high-order numerical magnetohydrodynamics (MHD) solver built upon a novel non-linear entropy stable numerical flux function that supports eight travelling wave solutions. By construction the solver conserves mass, momentum, and energy and is entropy stable. The method is designed to treat the divergence-free constraint on the magnetic field in a similar fashion to a hyperbolic divergence cleaning technique. The solver described herein is especially well-suited for flows involving strong discontinuities. Furthermore, we present a new formulation to guarantee positivity of the pressure. We present the underlying theory and implementation of the new solver into the multi-physics, multi-scale adaptive mesh refinement (AMR) simulation code FLASH (http://flash.uchicago.edu). The accuracy, robustness and computational efficiency is demonstrated with a number of tests, including comparisons to available MHD implementations in FLASH.

Magnetic helicity at early times

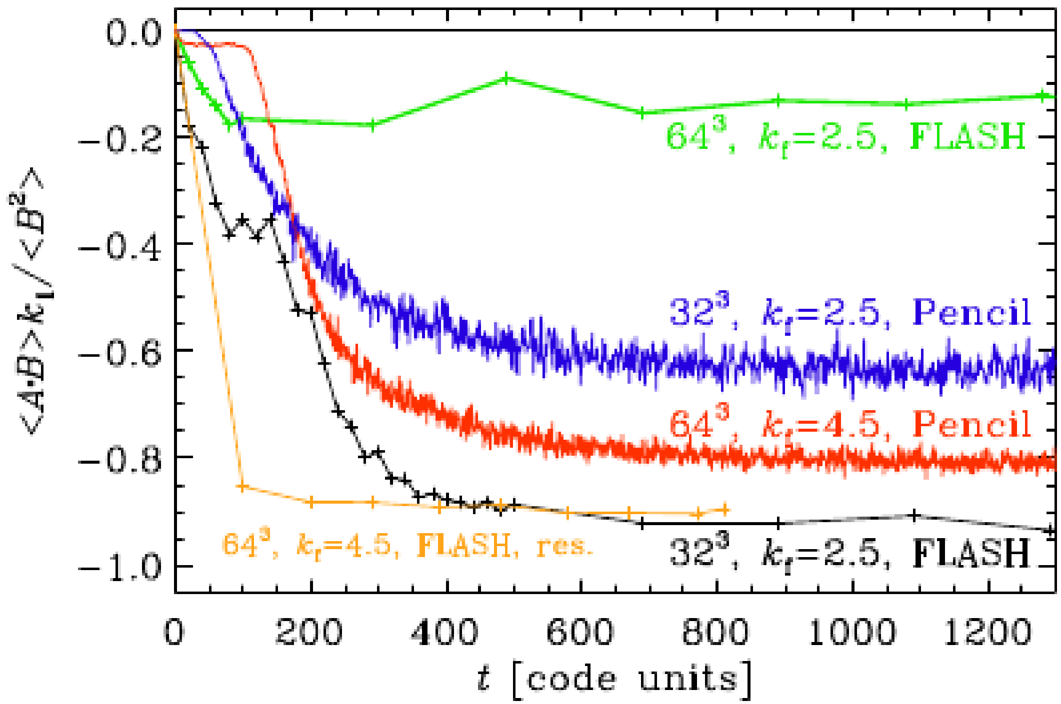

FIG. 14.— Evolution of the fractional magnetic helicity for the case with 32^3 mesh points, $k_f/k_1 = 2.5$, and $\eta^{\rm eff} = 5 \times 10^{-5}$ (black line), compared with the evolution in DNS with 32^3 mesh points, $k_f/k_1 = 2.5$, and $\eta = 5 \times 10^{-5}$ (blue). Also shown are a DNS with 64^3 mesh points ($k_f/k_1 = 4.5$, $\eta = 5 \times 10^{-5}$, red line), and a solution with FLASH with explicit resistivity ($k_f/k_1 = 4.5$, $\eta = 5 \times 10^{-5}$, orange line).

Small Lorentz factors, γ~1

$$\frac{\partial \ln \rho}{\partial t} = -\frac{4}{3}(\boldsymbol{\nabla}\cdot\boldsymbol{u}+\boldsymbol{u}\cdot\boldsymbol{\nabla}\ln\rho) + \frac{1}{\rho}\left[\boldsymbol{u}\cdot(\boldsymbol{J}\times\boldsymbol{B})+\eta\boldsymbol{J}^2\right],$$

$$\frac{\partial \boldsymbol{u}}{\partial t} = -\boldsymbol{u}\cdot\boldsymbol{\nabla}\boldsymbol{u}+\frac{\boldsymbol{u}}{3}(\boldsymbol{\nabla}\cdot\boldsymbol{u}+\boldsymbol{u}\cdot\boldsymbol{\nabla}\ln\rho) - \frac{\boldsymbol{u}}{\rho}\left[\boldsymbol{u}\cdot(\boldsymbol{J}\times\boldsymbol{B})+\eta\boldsymbol{J}^2\right]-\frac{1}{4}\boldsymbol{\nabla}\ln\rho + \frac{3}{4\rho}\boldsymbol{J}\times\boldsymbol{B}+\frac{2}{\rho}\boldsymbol{\nabla}\cdot(\rho\nu\mathsf{S})+\boldsymbol{\mathcal{F}},$$

$$\frac{\partial \boldsymbol{B}}{\partial t} = \nabla\times(\boldsymbol{u}\times\boldsymbol{B}-\eta\boldsymbol{J}+\boldsymbol{\mathcal{E}}),$$

Resulting stress

$$T_{ij} = (p+\rho)\,\gamma^2 u_i u_j - B_i B_j + (p + \boldsymbol{B}^2/2)\delta_{ij}$$

- Drives GWs
- Only transverse-traceless (TT) projection matters

$$\left(\frac{\partial^2}{\partial t^2} - c^2\nabla^2\right) h_{ij}^{\mathrm{TT}}(\boldsymbol{x}, t) = \frac{16\pi G}{a(t)c^2} T_{ij}^{\mathrm{TT}}(\boldsymbol{x}, t)$$

Just solve like other PDEs

$$\frac{\partial h_{+/\times}}{\partial t} = g_{+/\times}$$

$$\frac{\partial g_{+/\times}}{\partial t} = \nabla^2 h_{+/\times} + S_{+/\times}$$

$$\hat{S}_{ij} = \hat{S}_+ \, e^+_{ij} + \hat{S}_\times \, e^\times_{ij}$$

$$\hat{S}_+ = \tfrac{1}{2} e^+_{ij} \, \hat{S}_{ij}$$

$$\hat{S}_\times = \tfrac{1}{2} e^\times_{ij} \, \hat{S}_{ij}$$

- Two 1st order eqns
- No artificial diff needed (no shocks)
- TT projection on the source
- Alternatively: TT projection only for diagnostics

"Usual" 3rd order Runge-Kutta

$$\begin{pmatrix} h_{ij} \\ h'_{ij} \end{pmatrix}_{t+\delta t} \equiv \boldsymbol{q}_i, \quad \text{where} \quad \boldsymbol{q}_i = \boldsymbol{q}_{i-1} + \beta_i \boldsymbol{w}_i, \quad \boldsymbol{w}_i = \alpha_i \boldsymbol{w}_{i-1} + \delta t \boldsymbol{Q}_{i-1}, \quad \text{(approach I)}.$$

with $\alpha_1 = 0$, $\alpha_2 = -5/9$, $\alpha_3 = -153/128$, $\beta_1 = 1/3$, $\beta_2 = 15/16$, $\beta_3 = 8/15$, and

$$\boldsymbol{q}_{i-1} \equiv \begin{pmatrix} h_{ij} \\ h'_{ij} \end{pmatrix}_t, \quad \boldsymbol{Q}_{i-1} \equiv \begin{pmatrix} h'_{ij} \\ c^2 \nabla^2 h_{ij} + \mathcal{G} T_{ij} \end{pmatrix}_t .$$

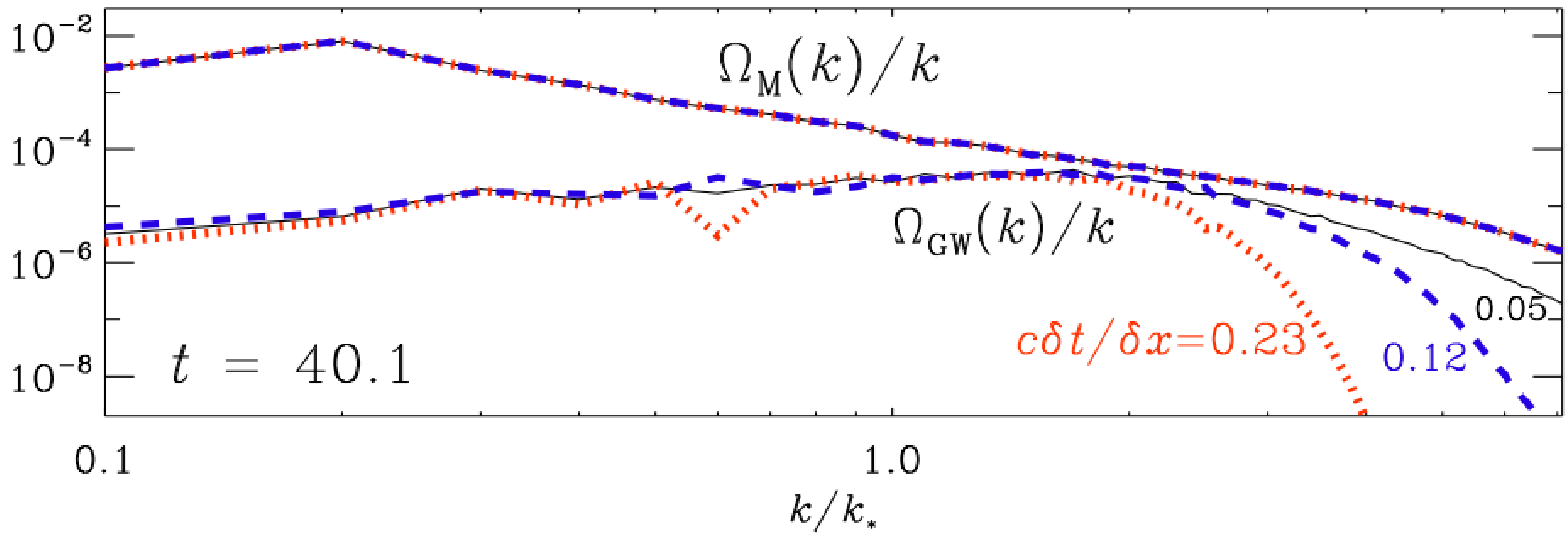

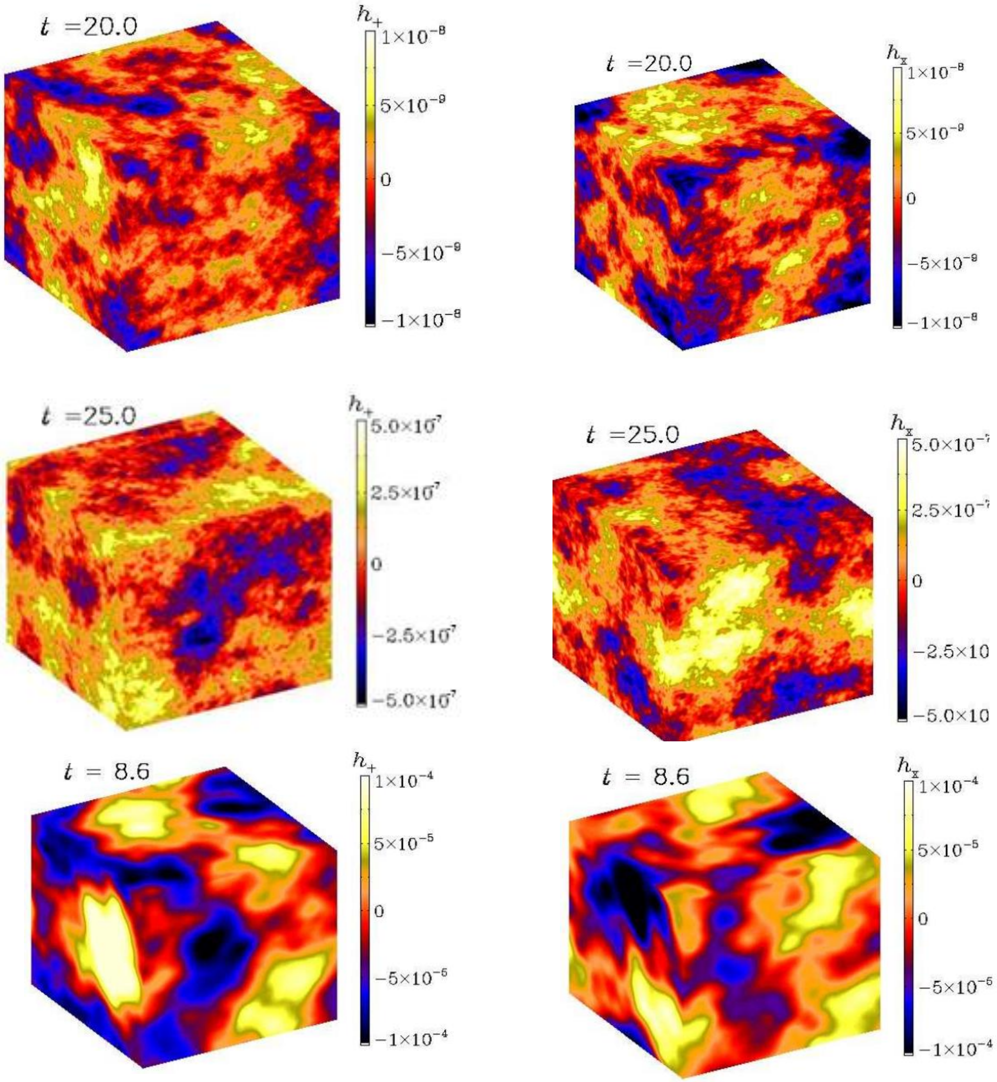

$k_M/k_H = 300$

$k_M/k_H = 60$

$k_M/k_H = 2$

“Exact” between 2 time steps

$$\begin{pmatrix} \omega\tilde{h} - \omega^{-1}\mathcal{G}\tilde{T} \\ \tilde{h}' \end{pmatrix}_{+,\times}^{t+\delta t} = \begin{pmatrix} \cos\omega\delta t & \sin\omega\delta t \\ -\sin\omega\delta t & \cos\omega\delta t \end{pmatrix} \begin{pmatrix} \omega\tilde{h} - \omega^{-1}\mathcal{G}\tilde{T} \\ \tilde{h}' \end{pmatrix}_{+,\times}^{t}$$

```
!
!  compute omega (but assume c=1), omega*t, etc.
!
          om12=one_over_k2
          om1=sqrt(om12)
          om=1./om1
          omt1=1./(om*t)
!
!  compute cos(om*dt) and sin(om*dt) to get from one timestep to the next.
!
          cosot=cos(om*dt)
          sinot=sin(om*dt)
!
!  Solve wave equation for hT and gT from one timestep to the next.
!
          coefAre=(hhTre-om12*S_T_re(ikx,iky,ikz))
          coefAim=(hhTim-om12*S_T_im(ikx,iky,ikz))
          coefBre=ggTre*om1
          coefBim=ggTim*om1
          f(nghost+ikx,nghost+iky,nghost+ikz,ihhT  )=coefAre*cosot+coefBre*sinot+om12*S_T_re(ikx,iky,ikz)
          f(nghost+ikx,nghost+iky,nghost+ikz,ihhTim)=coefAim*cosot+coefBim*sinot+om12*S_T_im(ikx,iky,ikz)
          f(nghost+ikx,nghost+iky,nghost+ikz,iggT  )=coefBre*cosot*om-coefAre*om*sinot
          f(nghost+ikx,nghost+iky,nghost+ikz,iggTim)=coefBim*cosot*om-coefAim*om*sinot
!
```

Auxiliary arrays

```
!
!  Compute exact solution for hT, hX, gT, and gX in Fourier space.
!
            hhTre=f(nghost+ikx,nghost+iky,nghost+ikz,ihhT  )
            hhXre=f(nghost+ikx,nghost+iky,nghost+ikz,ihhX  )
            hhTim=f(nghost+ikx,nghost+iky,nghost+ikz,ihhTim)
            hhXim=f(nghost+ikx,nghost+iky,nghost+ikz,ihhXim)
!
            ggTre=f(nghost+ikx,nghost+iky,nghost+ikz,iggT  )
            ggXre=f(nghost+ikx,nghost+iky,nghost+ikz,iggX  )
            ggTim=f(nghost+ikx,nghost+iky,nghost+ikz,iggTim)
            ggXim=f(nghost+ikx,nghost+iky,nghost+ikz,iggXim)
!
```

```
IDL> pc_read_var,obj=var
% PC_VARCONTENT: Dimensions of "iStr" do not fit to number of entries in "index.pro"!
% Error occurred at: PC_VARCONTENT     329 /home/brandenb/pencil-code/idl/read/pc_varcontent.pro
%                    PC_READ_VAR       376 /home/brandenb/pencil-code/idl/read/pc_read_var.pro
%                    $MAIN$              7 /home/brandenb/pencil-code/sayan/GW/idl/pvar.pro
% Execution halted at: $MAIN$              7 /home/brandenb/pencil-code/sayan/GW/idl/pvar.pro
```

```fortran
!
!   Register ggT and ggX as auxiliary arrays
!   May want to do this only when Fourier transform is enabled.
!
      if (lggTX_as_aux) then
        call farray_register_auxiliary('ggT',iggT)
        call farray_register_auxiliary('ggX',iggX)
        call farray_register_auxiliary('ggTim',iggTim)
        call farray_register_auxiliary('ggXim',iggXim)
      endif
!
      if (lhhTX_as_aux) then
        call farray_register_auxiliary('hhT',ihhT)
        call farray_register_auxiliary('hhX',ihhX)
        call farray_register_auxiliary('hhTim',ihhTim)
        call farray_register_auxiliary('hhXim',ihhXim)
      endif
!
      if (lStress_as_aux) then
        call farray_register_auxiliary('StT',iStressT)
        call farray_register_auxiliary('StX',iStressX)
        call farray_register_auxiliary('StTim',iStressTim)
        call farray_register_auxiliary('StXim',iStressXim)
        call farray_register_auxiliary('Str',iStress_ij,array=6)
      endif
!
```

Projection

$$\tilde{h}_{ij}^{\mathrm{TT}}(\boldsymbol{k}, t) = (P_{il}P_{jm} - \tfrac{1}{2}P_{ij}P_{lm})\tilde{h}_{lm}(\boldsymbol{k}, t). \tag{8}$$

Next, we compute the linear polarisation basis,

$$e_{ij}^{+}(\boldsymbol{k}) = e_i^1 e_j^1 - e_i^2 e_j^2, \quad e_{ij}^{\times}(\boldsymbol{k}) = e_i^1 e_j^2 + e_i^2 e_j^1, \tag{9}$$

where $\boldsymbol{e}^1$ and $\boldsymbol{e}^2$ are unit vectors perpendicular to $\boldsymbol{k}$ and perpendicular to each other. This polarisation basis has the following orthogonality property

$$e_{ij}^{+}(\boldsymbol{k})e_{ij}^{+}(\boldsymbol{k}) = e_{ij}^{\times}(\boldsymbol{k})e_{ij}^{\times}(\boldsymbol{k}) = 2, \quad e_{ij}^{+}(\boldsymbol{k})e_{ij}^{\times}(\boldsymbol{k}) = 0. \tag{10}$$

Thus, the strains are decomposed into the two independent $+$ and $\times$ modes, such that $\tilde{h}_{ij}^{\mathrm{TT}}(\boldsymbol{k}, t) = e_{ij}^{+}(\boldsymbol{k})\tilde{h}_{+}(\boldsymbol{k}, t) + e_{ij}^{\times}(\boldsymbol{k})\tilde{h}_{\times}(\boldsymbol{k}, t)$, with

$$\tilde{h}_{+}(\boldsymbol{k}, t) = \tfrac{1}{2}e_{ij}^{+}(\boldsymbol{k})\tilde{h}_{ij}^{\mathrm{TT}}(\boldsymbol{k}, t), \quad \tilde{h}_{\times}(\boldsymbol{k}, t) = \tfrac{1}{2}e_{ij}^{\times}(\boldsymbol{k})\tilde{h}_{ij}^{\mathrm{TT}}(\boldsymbol{k}, t). \tag{11}$$

Projection

for $|k_1| < \min(|k_2|, |k_3|)$:

$$\boldsymbol{e}^1 = \mathrm{sgn}(\boldsymbol{k})(0, -\hat{k}_3, \hat{k}_2), \quad \boldsymbol{e}^2 = (\hat{k}_2^2 + \hat{k}_3^2, -\hat{k}_1\hat{k}_2, -\hat{k}_1\hat{k}_3), \tag{14}$$

for $|k_2| < \min(|k_3|, |k_1|)$:

$$\boldsymbol{e}^1 = \mathrm{sgn}(\boldsymbol{k})(\hat{k}_3, 0, -\hat{k}_1), \quad \boldsymbol{e}^2 = (-\hat{k}_2\hat{k}_1, \hat{k}_3^2 + \hat{k}_1^2, -\hat{k}_2\hat{k}_3), \tag{15}$$

for $|k_3| \leq \min(|k_1|, |k_2|)$:

$$\boldsymbol{e}^1 = \mathrm{sgn}(\boldsymbol{k})(-\hat{k}_2, \hat{k}_1, 0), \quad \boldsymbol{e}^2 = (-\hat{k}_3\hat{k}_1, -\hat{k}_3\hat{k}_2, \hat{k}_1^2 + \hat{k}_2^2), \tag{16}$$

where we define the sign of a general wavevector $\boldsymbol{k} = (k_1, k_2, k_3)$ in the following way

$$\mathrm{sgn}(\boldsymbol{k}) = \begin{cases} \mathrm{sgn}(k_3) & \text{if } k_3 \neq 0, \\ \mathrm{sgn}(k_2) & \text{if } k_3 = 0 \text{ and } k_2 \neq 0, \\ \mathrm{sgn}(k_1) & \text{if } k_2 = k_3 = 0, \end{cases} \tag{17}$$

Projection

$$\operatorname{sgn}(\boldsymbol{k}) = \begin{cases} \operatorname{sgn}(k_3) & \text{if } k_3 \neq 0, \\ \operatorname{sgn}(k_2) & \text{if } k_3 = 0 \text{ and } k_2 \neq 0, \\ \operatorname{sgn}(k_1) & \text{if } k_2 = k_3 = 0, \end{cases} \tag{17}$$

such that half of the wavevectors are considered positive and the other corresponding half of the wavevectors are considered negative. The way to choose which half of the wavevectors are positive is arbitrary and could be changed leading to the same final result.

Note that neither $\boldsymbol{e}^1$ nor $\boldsymbol{e}^2$ flip sign under the parity transformation $\boldsymbol{k} \to -\boldsymbol{k}$. The reason for the $\operatorname{sgn}(\boldsymbol{k})$ term is the following. The linear polarisation tensorial basis $e_{ij}^{+}(\boldsymbol{k})$ and $e_{ij}^{\times}(\boldsymbol{k})$ must be represented by even operators with respect to $\boldsymbol{k}$ to reproduce the required modes, as will be shown in next section with a simple example, a one-dimensional Beltrami field. Alternatively, without loss of generality, we could have defined $\boldsymbol{e}^1$ and $\boldsymbol{e}^2$ such that both flip sign under $\boldsymbol{k} \to -\boldsymbol{k}$ transformations, such that both $e_{ij}^{+}(\boldsymbol{k})$ and $e_{ij}^{\times}(\boldsymbol{k})$ tensors are even operators.

Projection

```
one_over_k2=1./ksqr
if(abs(k1)<abs(k2)) then
  if(abs(k1)<abs(k3)) then !(k1 is pref dir)
    e1=(/0.,-k3,+k2/)
    e2=(/k2sqr+k3sqr,-k2*k1,-k3*k1/)
  else !(k3 is pref dir)
    e1=(/k2,-k1,0./)
    e2=(/k1*k3,k2*k3,-(k1sqr+k2sqr)/)
  endif
else !(k2 smaller than k1)
  if(abs(k2)<abs(k3)) then !(k2 is pref dir)
    e1=(/-k3,0.,+k1/)
    e2=(/+k1*k2,-(k1sqr+k3sqr),+k3*k2/)
  else !(k3 is pref dir)
    e1=(/k2,-k1,0./)
    e2=(/k1*k3,k2*k3,-(k1sqr+k2sqr)/)
  endif
endif
e1=e1/sqrt(e1(1)**2+e1(2)**2+e1(3)**2)
e2=e2/sqrt(e2(1)**2+e2(2)**2+e2(3)**2)
Pij(1)=1.-k1sqr*one_over_k2
Pij(2)=1.-k2sqr*one_over_k2
Pij(3)=1.-k3sqr*one_over_k2
Pij(4)=-k1*k2*one_over_k2
Pij(5)=-k2*k3*one_over_k2
Pij(6)=-k3*k1*one_over_k2
```

```
!
!  possibility of swapping the sign
!
          sign_switch=1.
          if (lswitch_sign_e_X) then
            if (k3<0.) then
              sign_switch=-1.
              e_X=-e_X
            elseif (k3==0.) then
              if (k2<0.) then
                sign_switch=-1.
                e_X=-e_X
              elseif (k2==0.) then
                if (k1<0.) then
                  sign_switch=-1.
                  e_X=-e_X
                endif
              endif
            endif
          endif
!
```

“Exact” between 2 time steps

$$\begin{pmatrix} \omega\tilde{h} - \omega^{-1}\mathcal{G}\tilde{T} \\ \tilde{h}' \end{pmatrix}_{+,\times}^{t+\delta t} = \begin{pmatrix} \cos\omega\delta t & \sin\omega\delta t \\ -\sin\omega\delta t & \cos\omega\delta t \end{pmatrix} \begin{pmatrix} \omega\tilde{h} - \omega^{-1}\mathcal{G}\tilde{T} \\ \tilde{h}' \end{pmatrix}_{+,\times}^{t}$$

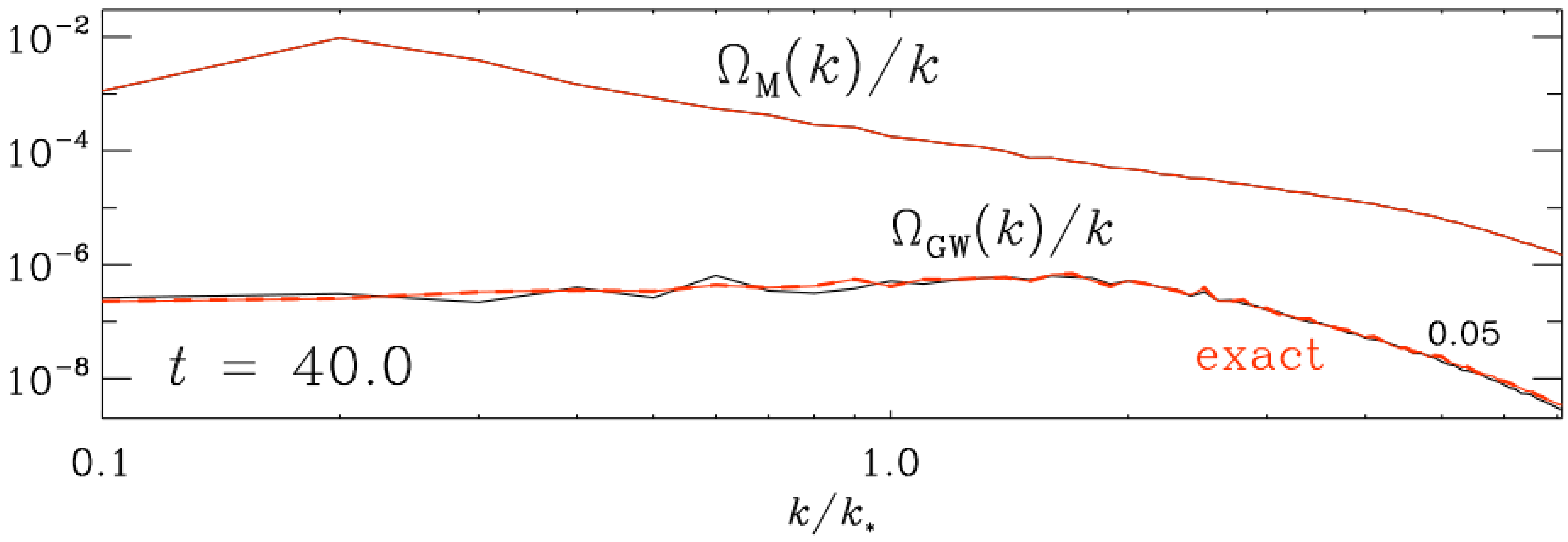

Sign switch for helicity diagnostics

```
sign_switch=1.
if (lswitch_sign_e_X) then
  if (k3<0.) then
    sign_switch=-1.
    e_X=-e_X
  elseif (k3==0.) then
    if (k2<0.) then
      sign_switch=-1.
      e_X=-e_X
    elseif (k2==0.) then
      if (k1<0.) then
        sign_switch=-1.
        e_X=-e_X
      endif
    endif
  endif
endif
```

```
!
!   Gravitational wave energy spectrum c(
!                                                !
          if (GWs_spec) then
            spectra%GWs(ik)=spectra%GWs(ik) &
               +f(nghost+ikx,nghost+iky,nghost+ikz,iggX  )**2 &
               +f(nghost+ikx,nghost+iky,nghost+ikz,iggXim)**2 &
               +f(nghost+ikx,nghost+iky,nghost+ikz,iggT  )**2 &
               +f(nghost+ikx,nghost+iky,nghost+ikz,iggTim)**2
            spectra%GWshel(ik)=spectra%GWshel(ik)+2*sign_switch*( &
               +f(nghost+ikx,nghost+iky,nghost+ikz,iggXim) &
               *f(nghost+ikx,nghost+iky,nghost+ikz,iggT  ) &
               -f(nghost+ikx,nghost+iky,nghost+ikz,iggX  ) &
               *f(nghost+ikx,nghost+iky,nghost+ikz,iggTim) )
          endif
!
```

Magnetic helicity → circular polarization of GWs

Beltrami field as an example

$$\boldsymbol{B} = \begin{pmatrix} 0 \\ \sigma \sin kx \\ \cos kx \end{pmatrix} \longrightarrow \boldsymbol{\nabla} \times \boldsymbol{B} = \begin{pmatrix} \partial_x \\ 0 \\ 0 \end{pmatrix} \times \begin{pmatrix} 0 \\ \sin kx \\ \cos kx \end{pmatrix} = k \begin{pmatrix} 0 \\ \sin kx \\ \cos kx \end{pmatrix} = k\boldsymbol{B}$$

Traceless-transverse

$$T_{ij}(x) = \mathcal{E}_{\mathrm{M}} \begin{pmatrix} 0 & 0 & 0 \\ 0 & -\cos 2kx & \sigma \sin 2kx \\ 0 & \sigma \sin 2kx & \cos 2kx \end{pmatrix}$$

Fully helical turbulence with positive or negative helicity

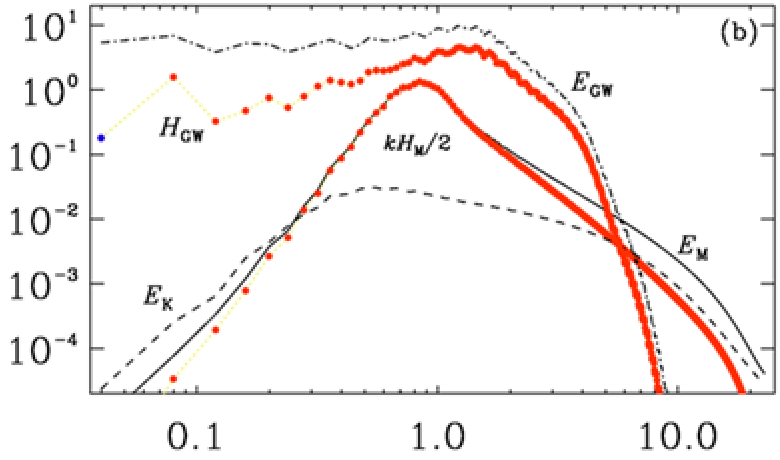

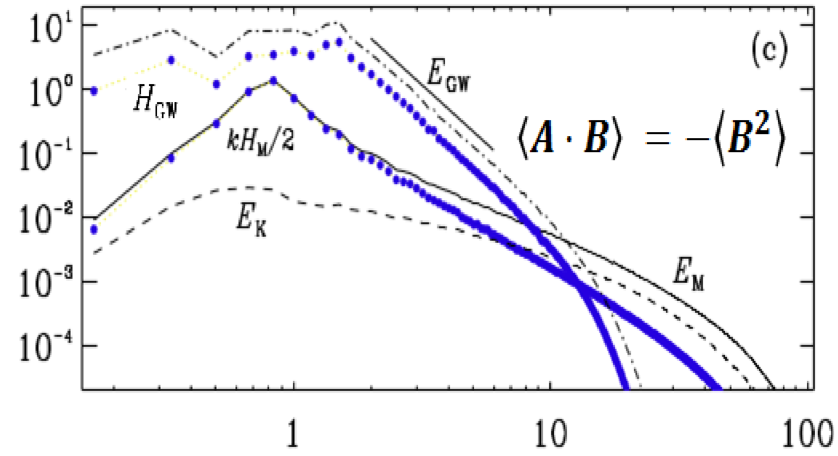

- Magnetic energy spectrum $\int E_M(k,t)\,dk = \langle \boldsymbol{B}^2 \rangle / 2$
- Positive helicity (red), negative (blue)
- GW energy spectra

GW polarization vs helicity

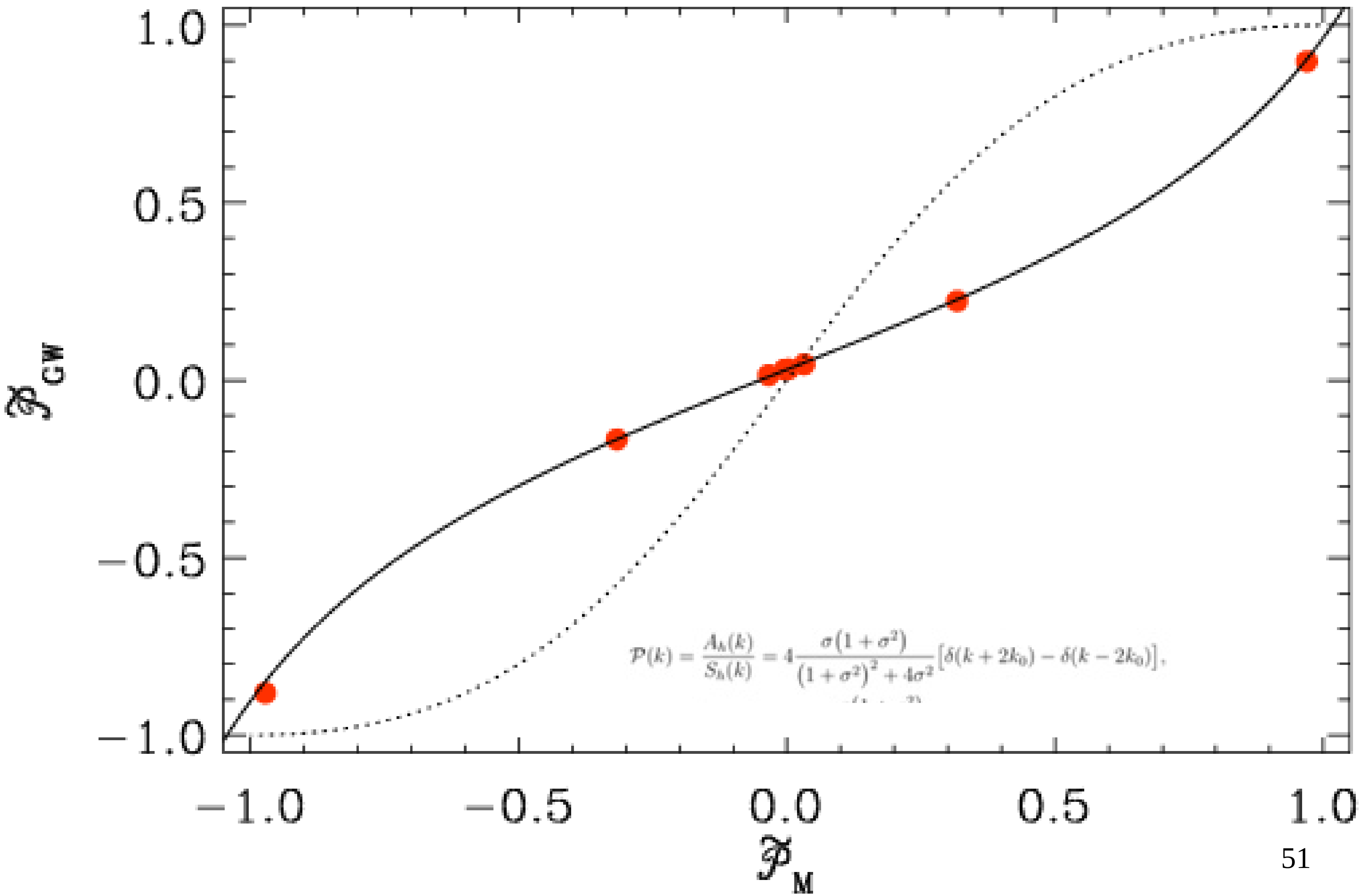

Correspondence of spectra

$$\left(\partial_{\bar{t}}^2 - c^2\nabla^2\right) h_{ij}(\boldsymbol{x},\bar{t}) = 6\, T_{ij}^{\mathrm{TT}}(\boldsymbol{x},\bar{t})/\bar{t}$$

$$T_{ij} = (p+\rho)\,\gamma^2 u_i u_j - B_i B_j + (p + \boldsymbol{B}^2/2)\delta_{ij}$$

- If spectral slope of *B* is -5/3, then
- Spectral slope of B^2 is -5/3-2 = -11/3
- But for slope 4, we don't get 4-2 = 2, but 0.

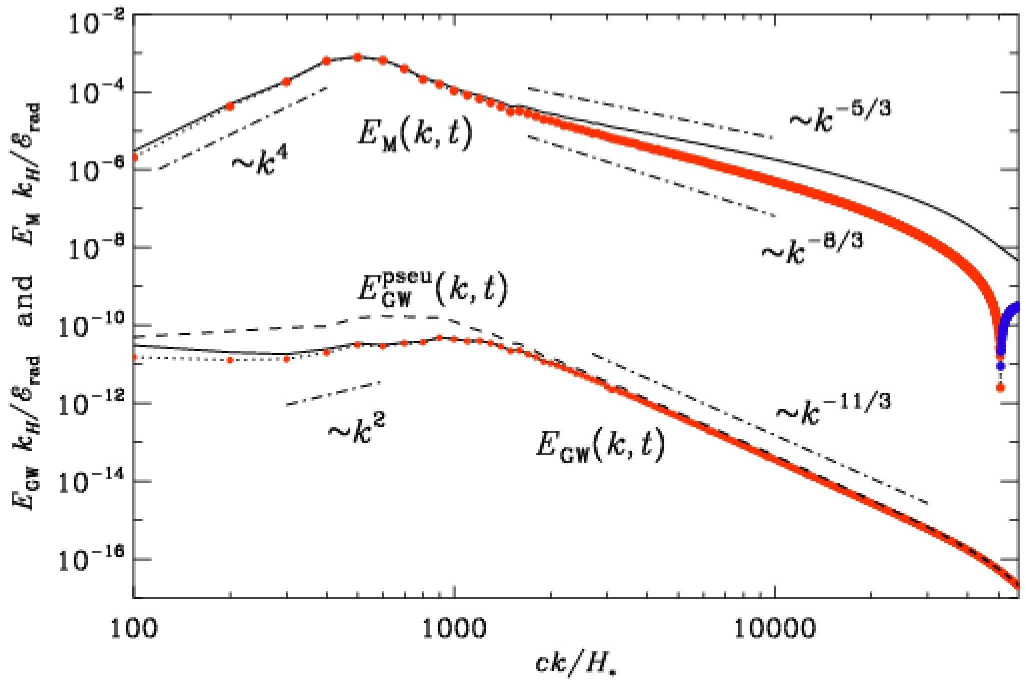

Spectra of the source

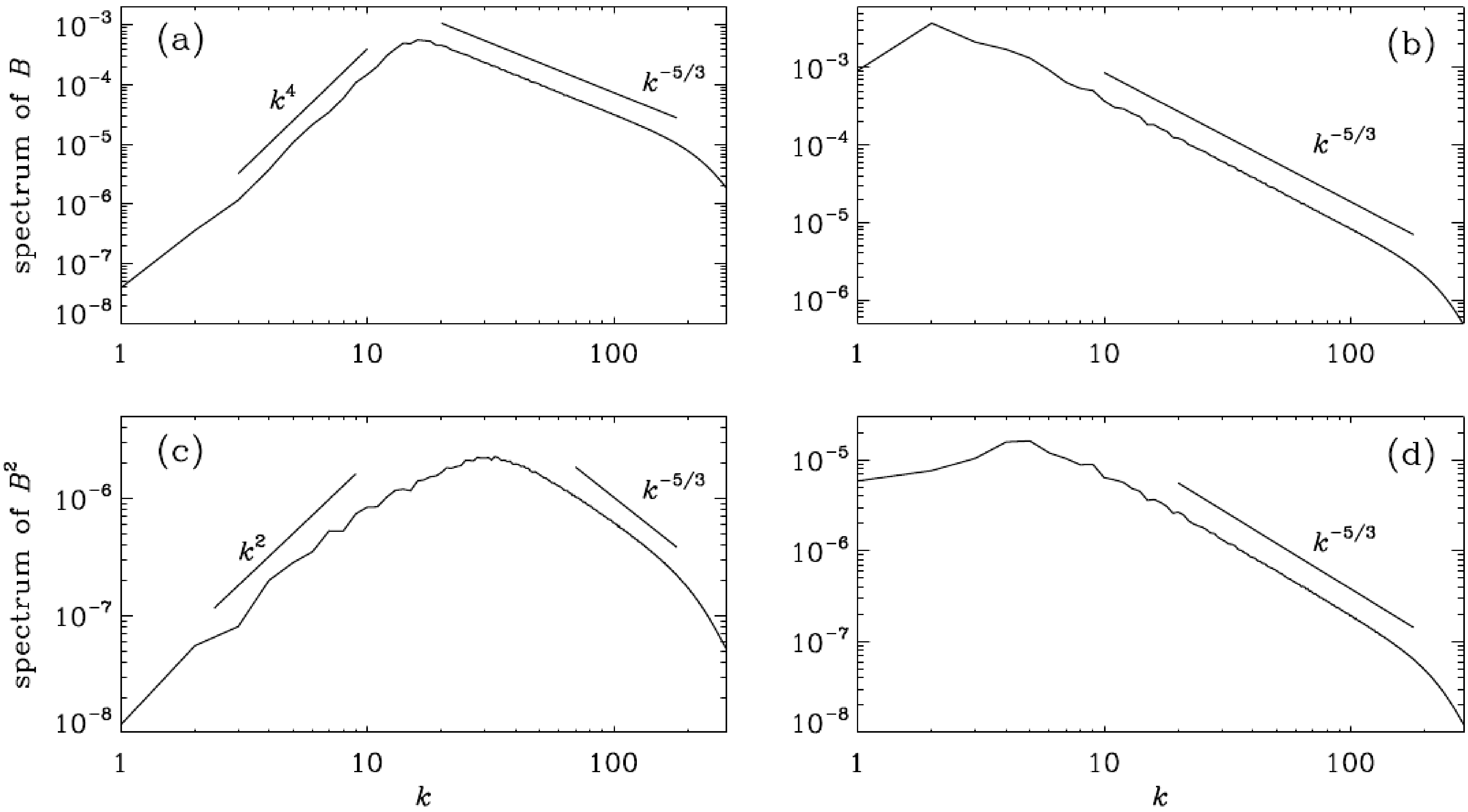

Experiments with scalar fields *s*

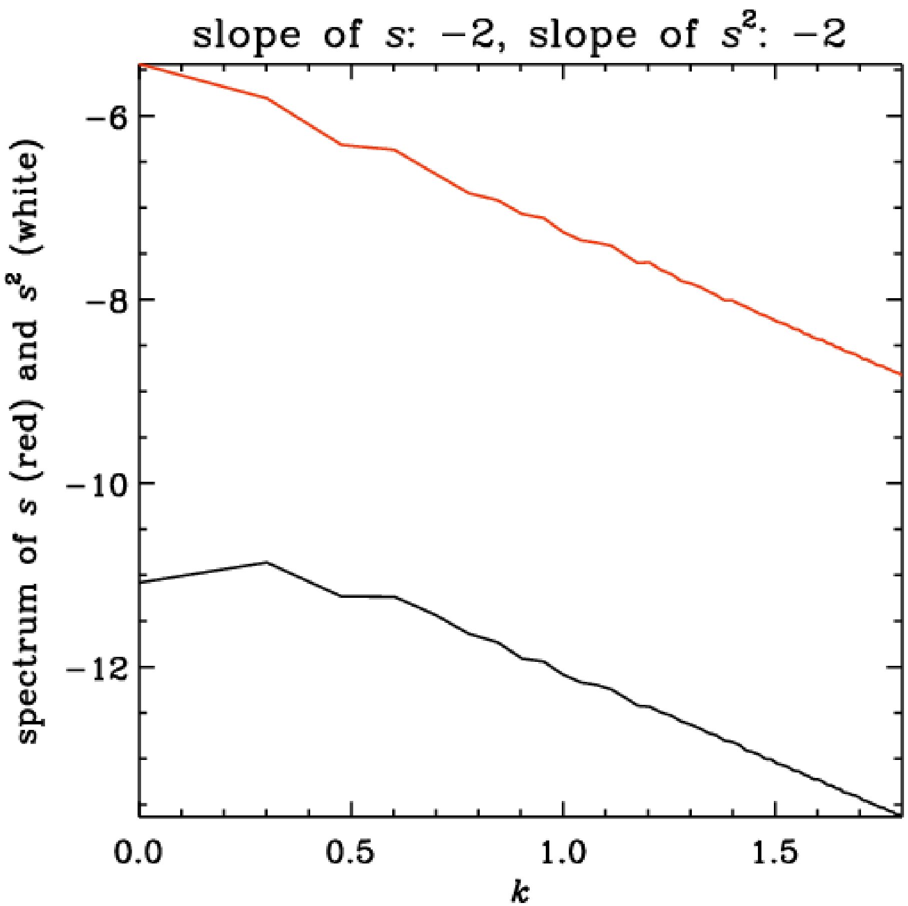

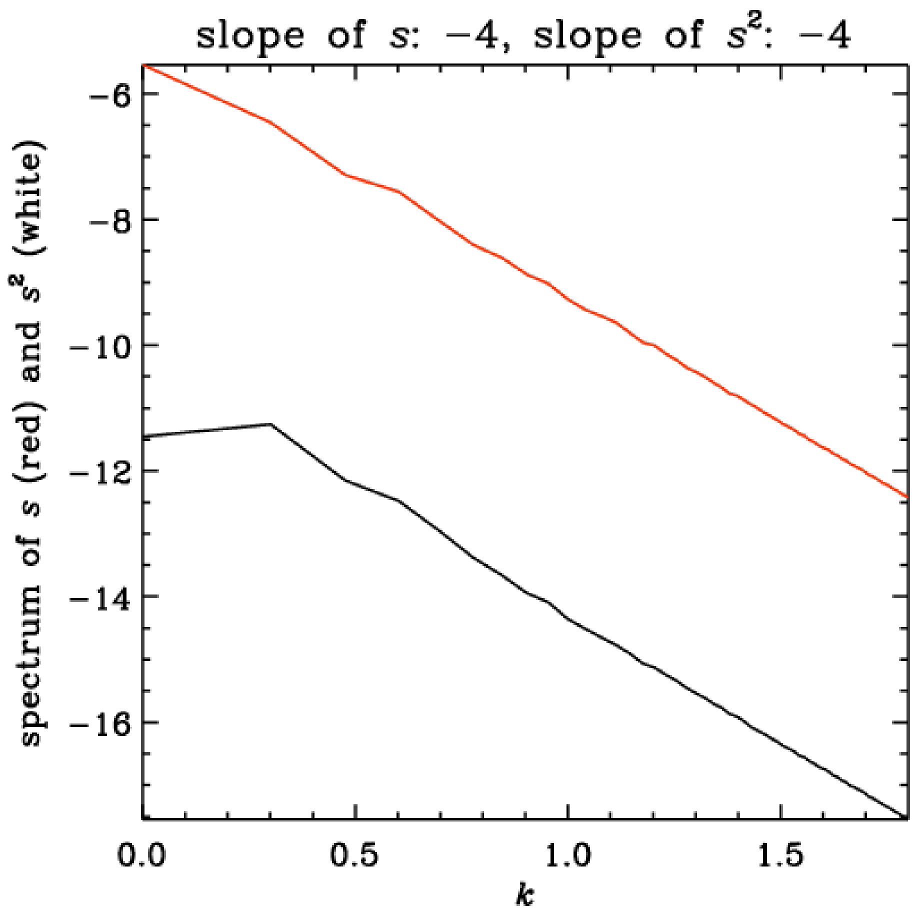

- Spectrum of source agrees with spectrum of d^2h/dt^2
- Spectrum of d^2h/dt^2 agrees with that of $k\,dh/dt$
- Therefore, spectrum of h is k^{-2} times that of source

Same for positive slopes

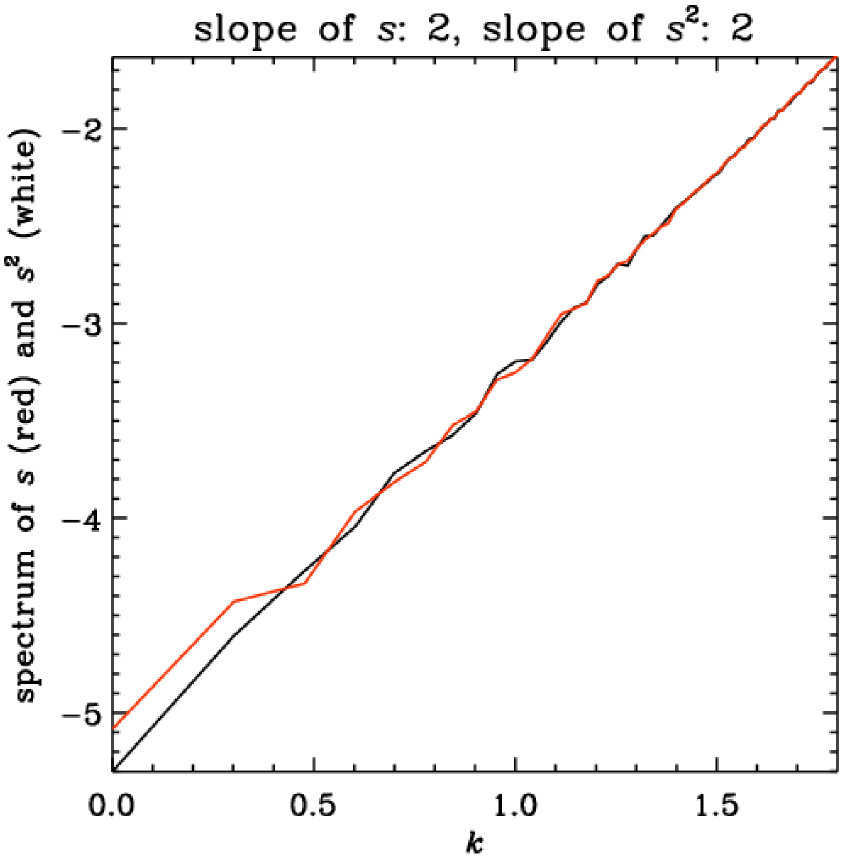

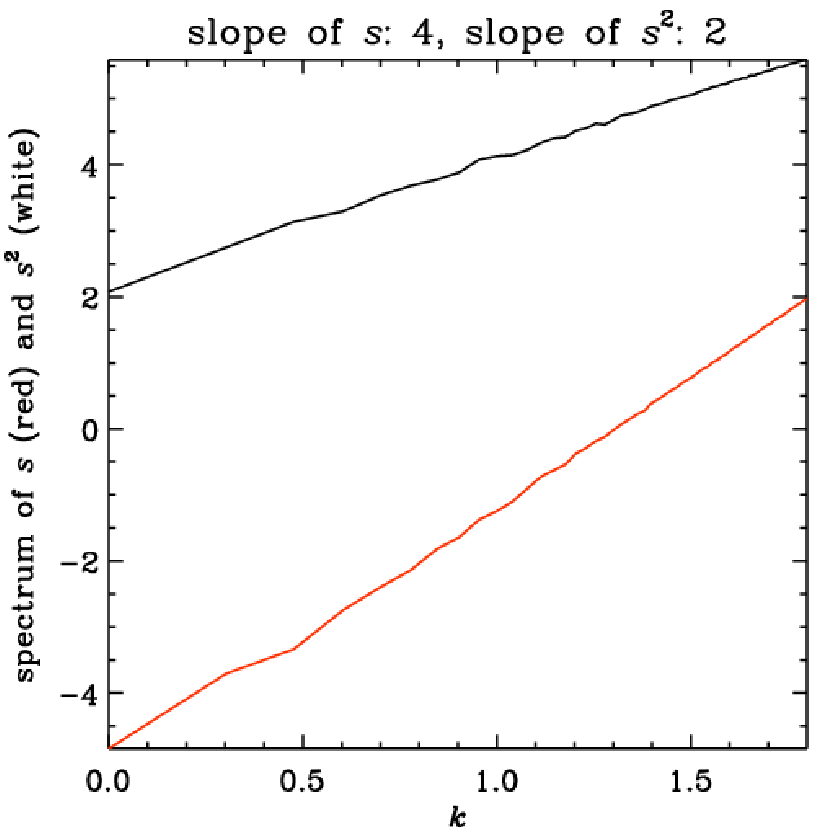

- k^2 spectrum is that of while noise (shell integrated!)
- Its square is also that of white noise
- Even a bluer spectrum becomes white again

Intermediate cases

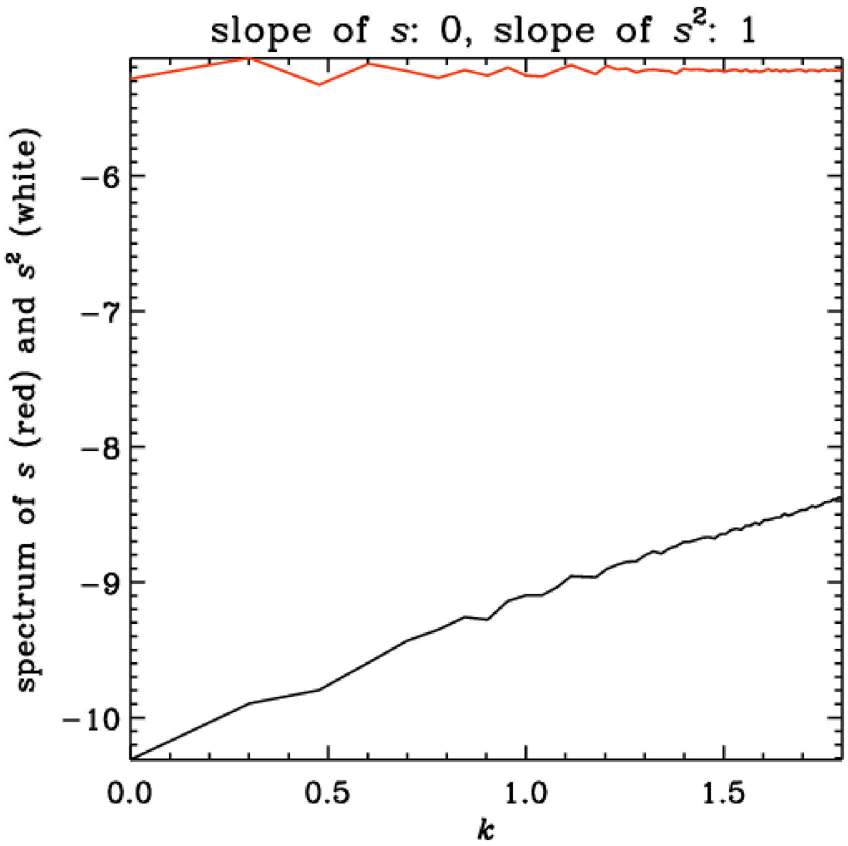

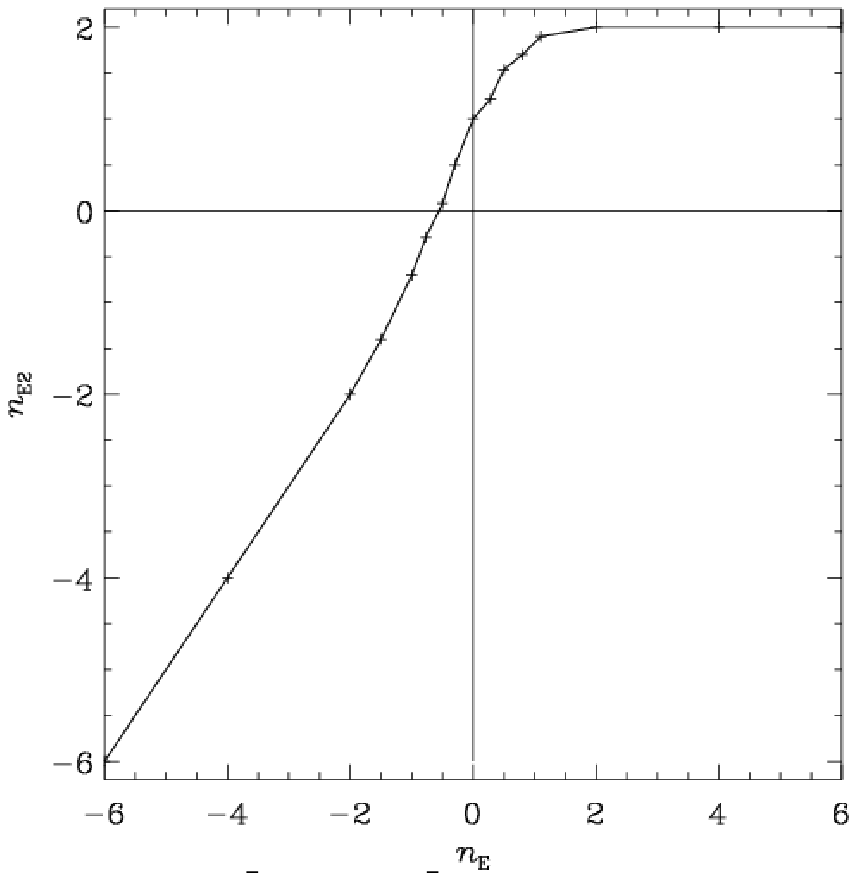

- For slopes btw -2 and 2: more complicated
- For red spectra (negative slope): same
- For blue spectra (steeper than 2): always 2 (white)

The Turbulent Stress Spectrum in the Inertial and Subinertial Ranges

Axel Brandenburg[1,2,3,4] and Stanislav Boldyrev[5,6]
[1] Nordita, KTH Royal Institute of Technology and Stockholm University, Roslagstullsbacken 23, SE-10691 Stockholm, Sweden
[2] Department of Astronomy, AlbaNova University Center, Stockholm University, SE-10691 Stockholm, Sweden
[3] JILA and Laboratory for Atmospheric and Space Physics, University of Colorado, Boulder, CO 80303, USA
[4] McWilliams Center for Cosmology & Department of Physics, Carnegie Mellon University, Pittsburgh, PA 15213, USA
[5] Department of Physics, University of Wisconsin—Madison, 1150 University Avenue, Madison, WI 53706, USA
[6] Space Science Institute, Boulder, CO 80301, USA
Received 2019 December 16; revised 2020 February 3; accepted 2020 February 17; published 2020 March 31

$$F(k) = 2\int_{-\infty}^{\infty} E(k')E(k-k')\frac{dk'}{2\pi},$$

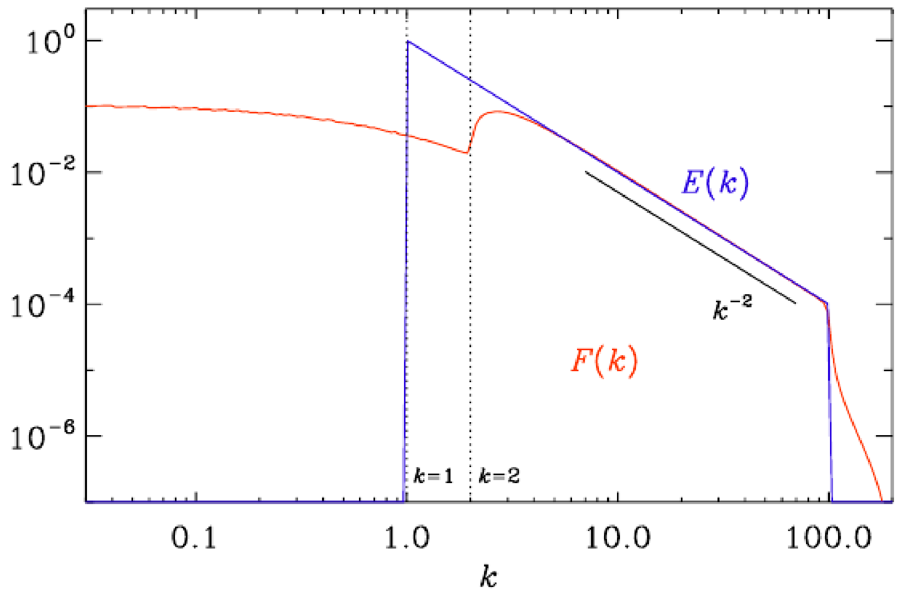

Figure 1. Numerically computed $F(k)$ (red) for $E(k) = k^{-2}$ (blue) for $1 \leqslant k \leqslant 100$ (and zero otherwise). The vertical solid and dotted lines mark $k = 1$ and 2, respectively.

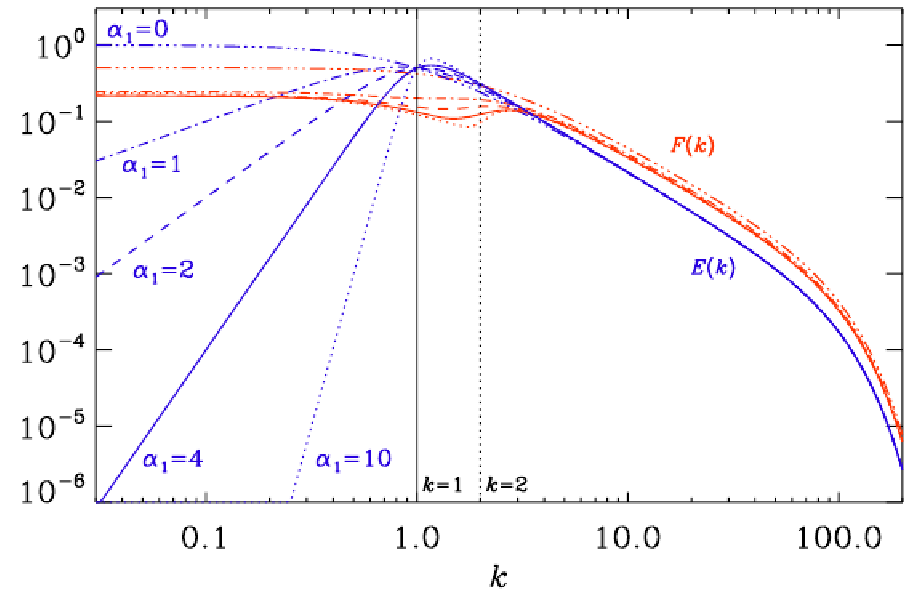

Figure 2. Similar to Figure 1, but for different subinertial range slopes: $\alpha_1 = 0$ (triple-dotted–dashed), 1 (dotted–dashed), 2 (dashed), 4 (solid), and 10 (dotted).

3-D and helical cases

$$F(k) = \int E(k')E(\kappa)\frac{k^2}{\kappa^2}\left[1 + \frac{(k\mu - k')^2}{\kappa^2}\right]\frac{dk'\,d\mu}{(2\pi)^3}$$

$$-\,2\int G(k')G(\kappa)\frac{k^2}{\kappa^2}\,\frac{k\mu - k'}{\kappa}\,\frac{dk'\,d\mu}{(2\pi)^3},$$

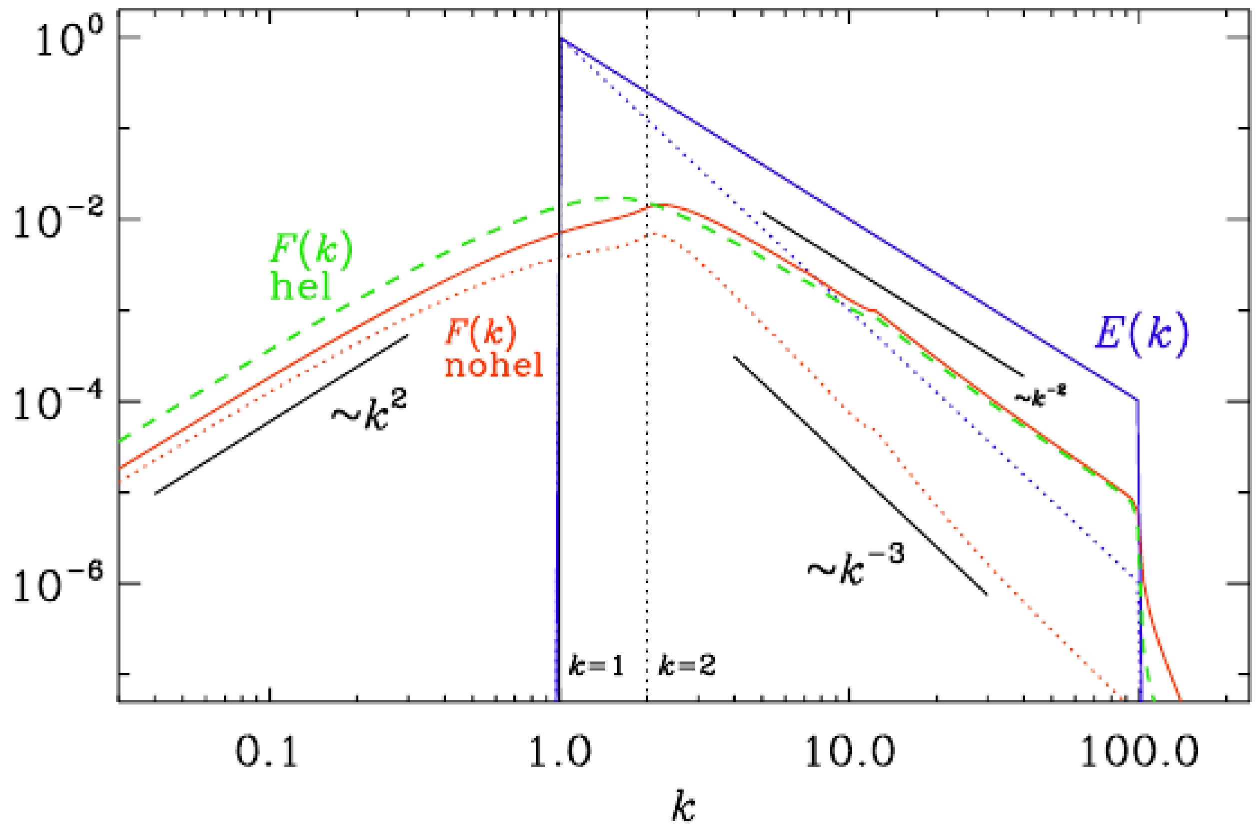

Non-abrupt end of driving

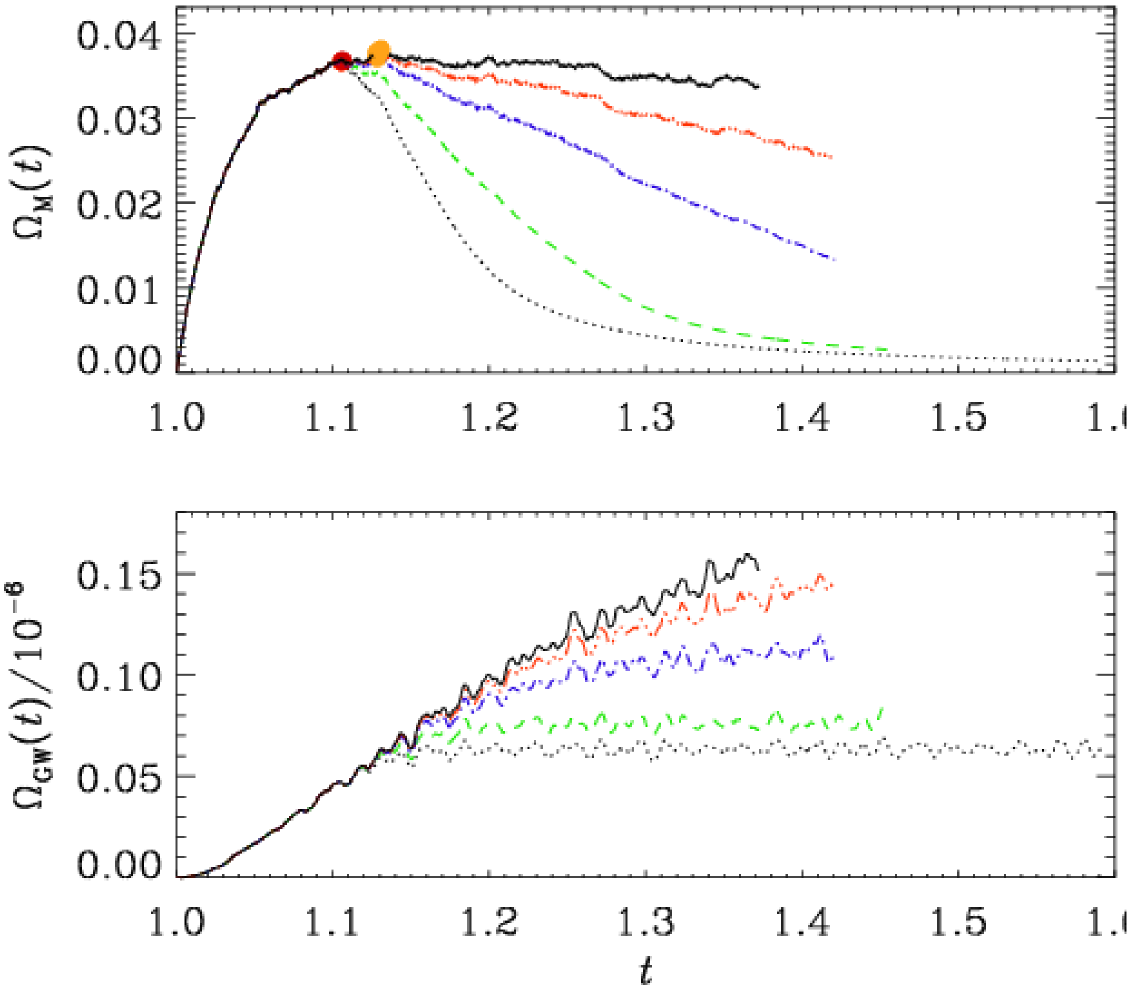

- Larger GW energy from graceful exit
- GW energy can be ~3x larger
- To understand slope-amplitude relation

Longer runs

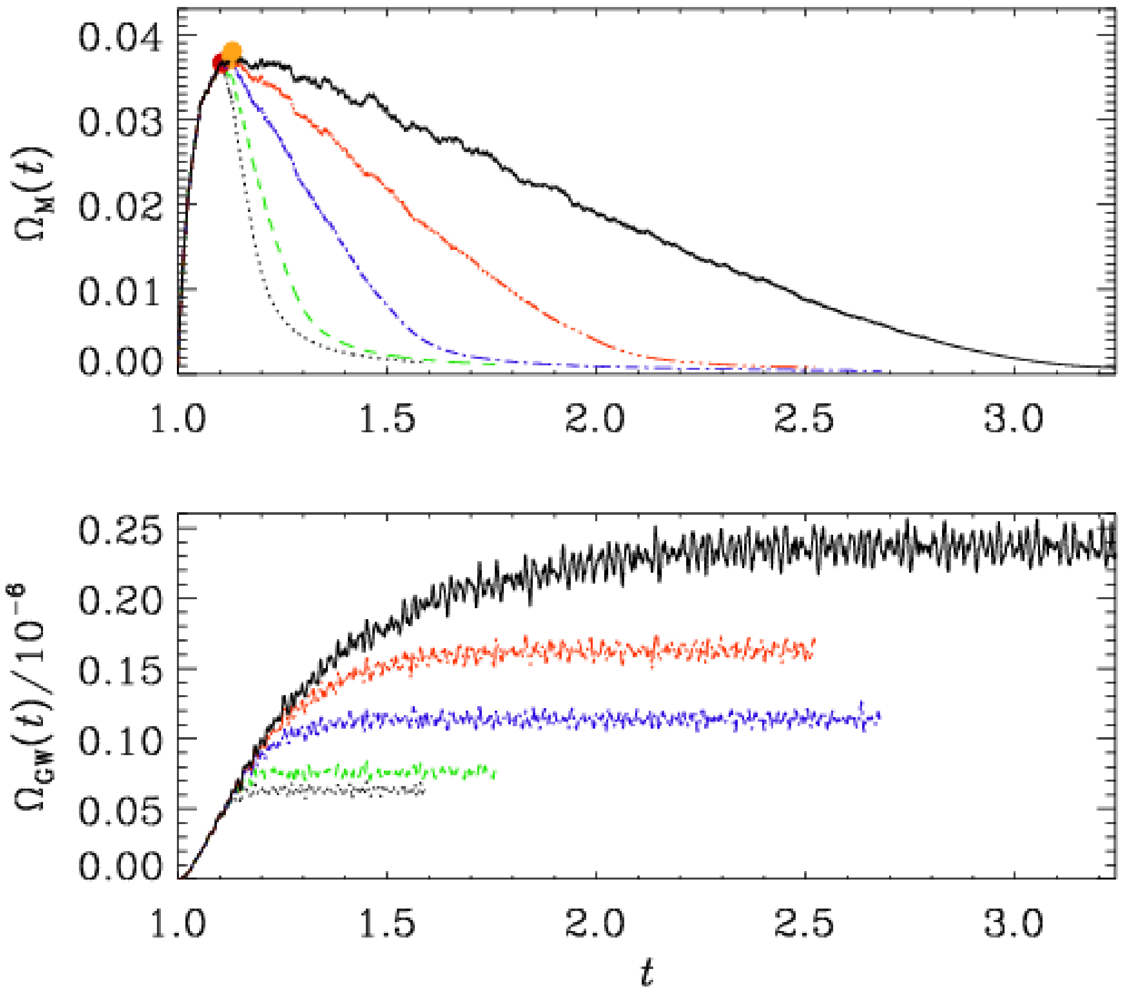

- Indeed: GW energy can be ~3x larger
- stops growing when Ω_{GW} drops below certain value
- About 20% of maximum?

GW energy & strain spectra

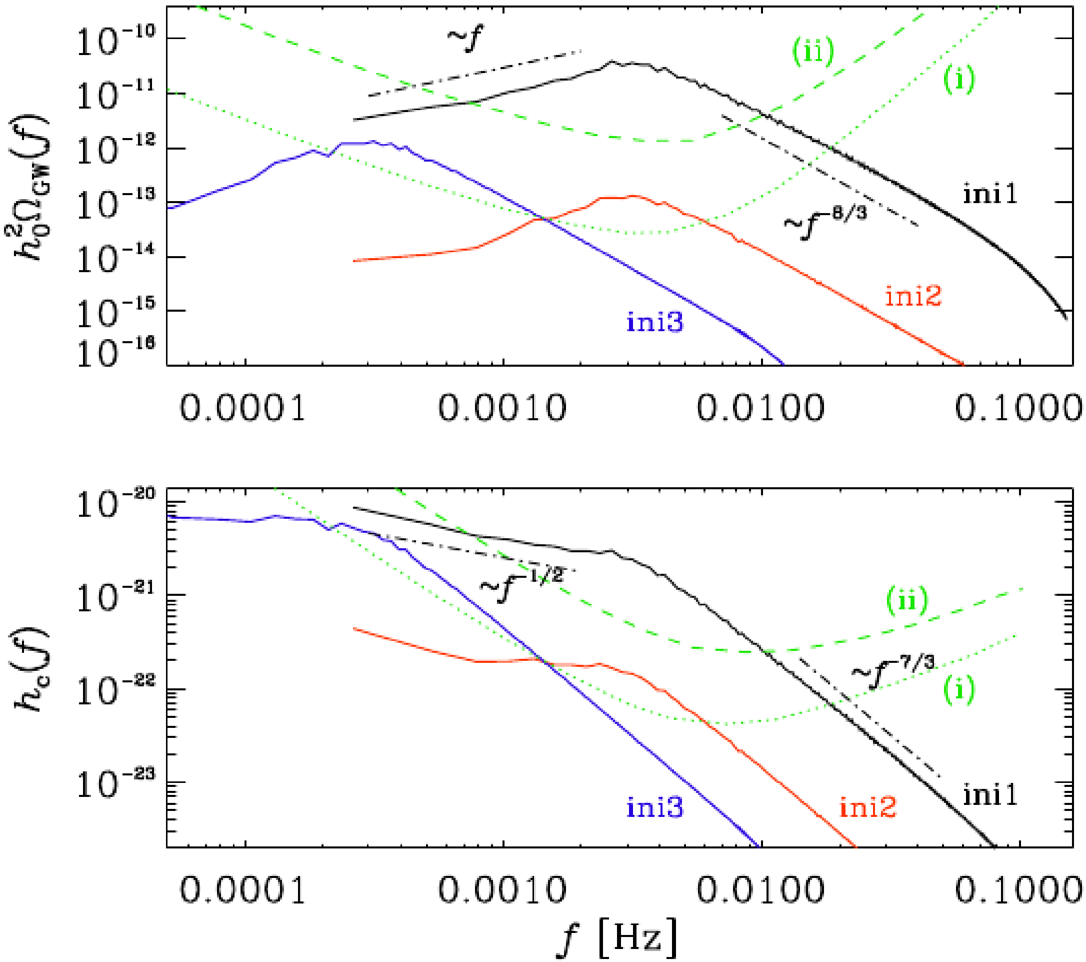

slope of	exp	new	Kol
E_M	4	—	$-5/3$
$E_\mathrm{GW} \propto S_{\dot h}$	2	0	$-11/3$
$\Omega_\mathrm{GW} \propto kS_{\dot h}$	3	1	$-8/3$
S_h	0	-2	$-17/3$
kS_h	1	-1	$-14/3$
h_c	$1/2$	$-1/2$	$-7/3$

- confirm also -8/3 and -7/3

Irrotational ←→ Vortical

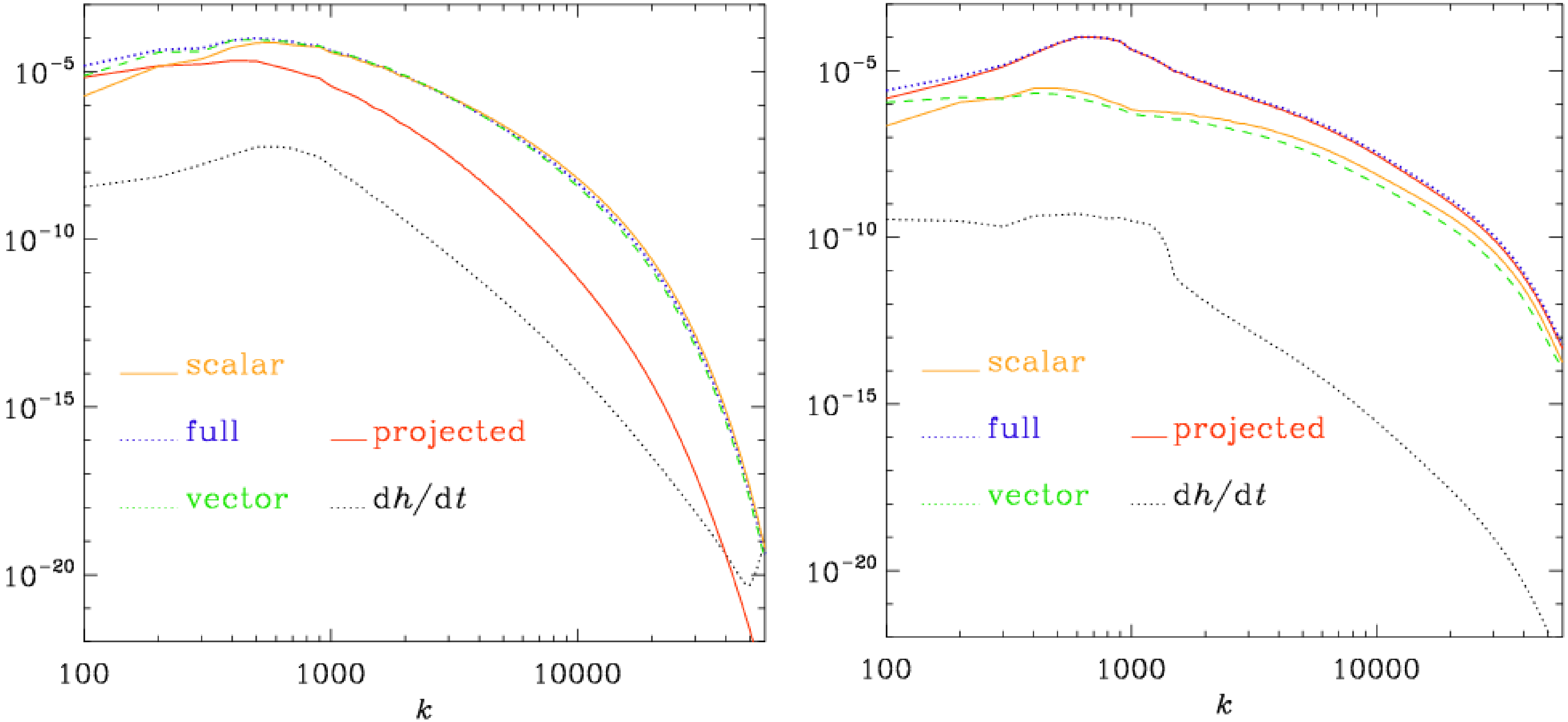

- Irrotational: scalar & vector dominant
- Vortical: subdominant, so full~projected!

Conclusion

- Pencil Code: GW advanced exactly
- For $E(k) \sim k^{-5/3}$ we get $\Omega(k) \sim k^{-8/3}$ and $h_c(k) \sim k^{-7/3}$
  - not -14/3 and -10/3
- but $E(k) \sim k^4$ leads to $\Omega(k) \sim k$ and $h_c(k) \sim k^{-1/2}$
  - not 3 and +1/2
- Vortical turbulence: vector & scalar modes weak
- Irrotational (acoustic) turbulence: they are strong, especially at small scales
  - GW generation coincides with onset of vorticity generation